Extracellular Vesicles From Adipose Stem Cells Prevent Muscle Damage and Inflammation in a Mouse Model of Hind Limb Ischemia: Role of Neuregulin-1

EXTRACELLULAR VESICLES FROM ADIPOSE STEM CELLS PREVENT MUSCLE DAMAGE AND INFLAMMATION IN A MOUSE MODEL OF HIND LIMB ISCHEMIA: ROLE OF NEUREGULIN-1

Federico Figliolini[1], Andrea Ranghino[2], Cristina Grange[2], Massimo Cedrino[1], Marta Tapparo[2], Claudia Cavallari[1], Andrea Rossi[2], Gabriele Togliatto[2], Saveria Femminò[2], Maria Vittoria Gugliuzza[2], Giovanni Camussi[2]* and Maria Felice Brizzi[2]*

[1]2i3T Scarl University of Turin, [2]Department of Medical Sciences, University of Turin, Turin, Italy

FF and AR contributed equally to the study

Running title: adipose stem cell-derived-EVs and HLI

Address correspondence to:

*Maria Felice Brizzi and Giovanni Camussi, Department of Medical Sciences, University of Turin, Corso Dogliotti 14, 10126, Turin, +39 011 6706653

mariafelice.brizzi@unito.it

giovanni.camussi@unito.it

Key words: muscle damage, inflammation, ASCs, HLI.

Subject codes: Pathophysiology, Stem cells, Peripheral vascular disease

Word count: 7497 words

Total number of figures and tables: 6 figures and 3 tables

TOC category: translational

TOC subcategory: Arteriosclerosis

ABSTRACT

Objective: Critical hind limb ischemia (CLI) is a severe consequence of peripheral artery disease. Surgical treatment does not prevent skeletal muscle impairment or improve long-term patient outcomes. The present study investigates the protective/regenerative potential and the mechanism of action of adipose stem cell-derived extracellular vesicles (ASC-EVs) in a mouse model of hind limb ischemia (HLI).

Approach and results: We demonstrated that ASC-EVs exert a protective effect on muscle damage by acting both on tissue microvessels and muscle cells. The genes involved in muscle regeneration were up-regulated in the ischemic muscles of ASC-EV-treated animals. MyoD expression has also been confirmed in satellite cells. This was followed by a reduction in muscle function impairment *in vivo*. ASC-EVs drive myoblast proliferation and differentiation in the *in vitro* ischemia/reoxigenation model. Moreover, ASC-EVs have shown an anti-apoptotic effect both *in vitro* and *in vivo*. Transcriptomic analyses have revealed that ASC-EVs carry a variety of pro-angiogenic mRNAs, while proteomic analyses have demonstrated an enrichment of neuregulin 1 (NRG1). A NRG1 blocking antibody used *in vivo* demonstrated that NRG1 is relevant to ASC-EV-induced muscle protection, vascular growth, and recruitment of inflammatory cells. Finally, bioinformatic analyses on 18 molecules that were commonly detected in ASC-EVs, including mRNAs and proteins, confirmed the enrichment of pathways involved in vascular growth and muscle regeneration/protection.

Conclusion: This study demonstrates that ASC-EVs display pro-angiogenic and skeletal muscle protective properties that are associated with their NRG1/mRNA cargo. We therefore propose that ASC-EVs are a useful tool for therapeutic angiogenesis and muscle protection.

ABBREVIATIONS AND ACRONYMS

ASC-EVs	Adipose stem cell-derived extracellular vesicles
BrdU	5-bromo-2-deoxyuridine
HMEC	Human microvascular endothelial cells
I/R	Ischemia/Reperfusion
Myf5	Myogenic factor 5
MyoD	Myoblast determination protein 1
NRG1	Neuregulin 1
p38MAPK	P38 mitogen-activated protein kinase
Pax7	Paired box protein 7
SCs	Satellite cells

INTRODUCTION

Critical limb ischemia (CLI) is a widespread disorder caused by the atherosclerosis of the peripheral arteries and is commonly found in patients with peripheral artery disease[1]. Reduced blood supply to the ischemic limb leads to skeletal muscle damage. The standard therapies, which are surgery and endovascular intervention, are not particularly effective, making patient management a significant economic burden[2,3]. The exponential growth of an aging population, the onset of diabetes and the high incidence of metabolic disease also pose a heavy social encumbrance, but are also driving forces for novel and effective therapeutic options. Regenerative medicine, and in particular cell-based therapy, has recently gained a great deal of attention[4]. Mesenchymal stem cells (MSCs), derived from a variety of sources, have been proposed to fulfill this role[4]. Bone-marrow derived MSCs are currently the most widely studied stem cells in regenerative medicine as they are known to home in and engraft injured tissues. However, special clinical interest has recently been shown in the use of adipose-derived stem cells (ASCs) in the ischemic setting as a range of useful properties, such as stimulation of angiogenesis, muscle regeneration and inflammation suppression,[5] have been attributed to them. Moreover, compared to MSCs, ASCs could be easily obtained. However, the inefficient engraftment of MSC and ASC suggests that their positive effects depend on their secretome (paracrine/autocrine hypothesis)[6].

Stem cell-derived extracellular vesicles (EVs) have emerged over the last decade in their role as important mediators of intercellular communication; they are involved in the transmission of signals between cells to regulate a wide range of biological actions[7]. Significant insight into the functional role that they play in a number of clinical settings has been gained[7]. In particular, it has been found that stem cell-derived EVs can mimic the effect of the cell of origin *via* the horizontal transfer of functional RNAs and proteins when systemically or locally administrated in regenerative medicine. The use of EVs for genetic information transfer has therefore also been proposed[8]. EVs that are released from stem cells can drive regenerative programs in cells that have survived injury in various pathological settings, such as heart ischemia/reperfusion injury,[9] and hepatectomy[10] models. miRNAs, mRNAs and proteins carried by EVs have been proven to favor angiogenesis and tissue regeneration.

Skeletal muscle damage is a hallmark of persistent ischemia/reperfusion (I/R) injury in patients with atherosclerosis of the peripheral arteries. In response to skeletal muscle damage, resident stem cells, known as satellite cells (SCs), are recruited and promptly participate in the regenerative processes by undergoing cell division. Myogenic regulatory factors Myf5 and MyoD are specific markers of the participation of differentiating myoblasts in the complex network of events during myogenesis[11]. However, tissue recovery after damage also requires an efficient blood supply, which is impaired in acute I/R injury. The pro-angiogenic properties of ASC-derived EVs have been reported to mainly depend on their miRNA cargo[12]. The present study investigates whether ASC-derived EVs may act on both vascular and skeletal muscle cells to protect muscles upon acute I/R damage and by which mechanism this may occur.

MATERIALS AND METHODS

The authors declare that all supporting data are available within the article and in the *online Data Supplement*

In vivo model of hind limb ischemia (HLI)

Animal studies were conducted in accordance with the Italian National Institute of Health Guide for the Care and Use of Laboratory Animals. All procedures were approved by the Ethics Committee of the University of Turin and the Italian Health Ministry (authorization number: 490/2015-PR). Mice were housed according to the Federation of European Laboratory Animal Science Association Guidelines. All experiments were performed in accordance with relevant guidelines and regulations. C57BL/6J male mice (Charles River Laboratories), aged 7 to 8 weeks were used. Since the female estrus cycle could introduce unexpected variables, only male mice have been used in this study. Hind limb ischemia was performed as previously described[13]. Two different ASC-EV administration routes were used in the preliminary study: route 1: ASC-EVs ($2x10^{10}$/mouse) were injected as detailed: $1x10^{10}$ administrated intravenously immediately after intervention (T0), $0.5x10^{10}$ via intramuscular injection on day 1 (T1) and again on day 2 (T2); route 2: ASC-EVs were injected intramuscularly at 1 $x10^{10}$ immediately after surgery (T0), and at $0.5x10^{10}$ at day 1 (T1) and day 2 (T2) (n=8/each group/protocol). Animals were sacrificed on either day 3 (T3) or day 7 (T7) for molecular and histological analyses (n=8/group). In selected experiments, ASC-EVs pretreated with a blocking antibody against neuregulin 1 (NRG1) (Raybiotech) were used (n=8).–Semi-quantitative estimations of foot damage [15](by repeated measures, analyzed using the ANOVA and Newman-Keuls Multiple Comparison tests) of foot damage were performed serially using the following classification: 3=dragging of foot (foot necrosis); 2=no dragging, but no plantar flexion (foot damage); 1=plantar flexion, but no toe flexion (toe damage); and 0=flexing the toes to resist gentle traction on the tail (no damage)[15]. In order to monitor blood flow, mice were placed on a heating plate at 37°C for 5 min, after anesthesia, to minimize temperature variations. Hind limb blood flow was measured using a Laser Doppler Blood–Perfusion (LDBP) analyzer (PeriScan PIM 3 System, Perimed, Stockholm, Sweden), immediately before and after surgery, and at days 3 and 7 after surgery. LDBP analysis was performed on hind limbs and feet. Blood flow was reported as changes in the laser frequency, using several color pixels. Images were analyzed to quantify blood flow using ROIs (regions of interest) that were drawn freehand. Hind limb blood flow was expressed as the ratio of left (ischemic) to right (non-ischemic) to avoid data variations that may be caused by ambient light and temperature[13]. To assess the area of muscle damage, at day 7 muscles were rapidly removed and incubated for 20 min at 37°C in 0.1% solution of nitro-blue tetrazolium in phosphate buffer. The necrotic mass was expressed as a percentage of total muscle mass (n=4 each/group protocol)[16]. Details are reported in the *online Data Supplement.*

Histological and immunofluorescence analyses

Gastrocnemius muscle sections from ischemic and normo-perfused limbs were stained with hematoxylin and eosin and Masson's trichrome for histological analysis. Images of all the injured areas of the ischemic limb sections were acquired for total muscle fiber counts. Random images from total, non-ischemic limb sections were used as controls. Data were quantified as percentage of damage area over total area. Capillary density was calculated as the number of capillaries per muscle fiber in Masson's trichrome sections. Ten randomly chosen microscopic fields, from three different sections in each tissue block, were examined and counted by two blind observers using Image J software. Capillary density was expressed as the number of capillaries per muscle fiber ±

SEM (Magnification: x400). Inflammatory cells in gastrocnemius muscles were quantified using immunofluorescence analyses on OCT embedded samples. Tissue slices (5 µm) were stained with a rat anti-mouse CD14 primary antibody (PharMingen). Fifteen randomly chosen microscopic fields, from three different sections in each tissue block, were examined for inflammatory cell count ~~by~~ (two blind observers). Inflammation was expressed as the number of CD14 positive cells per high power field (HPF) ± SEM (Magnification: x400).

Muscle cell proliferation was evaluated by immunohistochemistry. Gastrocnemious muscle sections ~~of~~ (paraffin-embedded samples) were stained with a monoclonal anti-proliferating Cell-Nuclear Antigen (anti-PCNA) antibody (Santa Cruz) (at day 7). Apoptosis was evaluated using the TUNEL assay (ApopTagOncor, Gaithersburg, MD. Number of PCNA-positive cells and TUNEL-positive nuclei were evaluated by counting the number of positive nuclei per field in 10 randomly chosen sections using ImageJ software. Details are reported in the *online Data Supplement.*

Isolation and characterization of ASC-EVs

Male-derived ASCs were purchased from Lonza and cultured in ADSC growth medium (Lonza) in T75 flasks. For EV isolation, ASCs (passage 2–7 and 60-70% of confluence) were washed several times with PBS (Lonza), to eliminate traces of serum and then cultured in alpha MEM (Lonza) with penicillin/streptomycin and L-glutamine (Sigma-Aldrich, St. Louis, MO) without FBS overnight (16 hours) in 5%CO2 incubator at 37°C. Cell culture supernatants (8 ml each T75 flask) were centrifuged twice at 4,000 rcf, for 10 min, at 4°C and submitted to microfiltration (0.22 µm PES from Meck Millipore, Tullagreen, Ireland) to eliminate cell debris and apoptotic bodies, and then ultracentrifuged at 100,000 rcf, for 2 hours, at 4°C in a Beckman Coulter Optima L-90K ultracentrifuge with rotor 70 Ti in polycarbonate tubes (355618) (Beckman Coulter, Indianapolis, IN). Pellets were resuspended in alpha MEM supplemented with 1% DMSO and stored at -80°C for further experiments. In selected experiments, ASC-EVs were either treated with anti-NRG1 blocking antibody (Raybiotech) 5 µg/ml for 1 hour at RT, or with trypsin 0.1X (0.025% w/v) for 1 hour at 37°C, then washed with PBS, re-ultracentrifuged at 100,000 rcf for 2 hours, at 4°C and resuspended, as previously described[13].

In order to perform Nanosight Tracking Analyses (NTA), ASC-EVs were diluted (1:200) in sterile saline solution (NaCl 0.9%) filtered with 0.1µm pore filter and analysed using a NanoSight NS300 equipped with NTA Analytical Software (Malvern Panalytical Ltd., Malvern, UK). The number of ASC-EVs released per cell was calculated as reported in the *online Data Supplement*.

Guava FACS analysis

The characterization of EV surface molecules was performed by GUAVA FACS analysis (GUAVA EasyCyte 8, Millipore) using MACSPlex exosome kit (Miltenyi biotech). Briefly, ASC-EVs were incubated with the antibody-coated capture Beads and subsequently ASC-EVs, bound to the MACSPlex Exosome Capture Beads, were labeled with the MACSPlex Exosome Detection Reagents containing different antibodies recognizing different surface markers. Control antibodies were also used. Consequently, the sandwich complexes formed among the MACSPlex Exosome Capture Bead, ASC-EVs, and the detection reagent were analyzed based on the fluorescence generated by the MACSPlex Exosome Capture Bead and the detection reagents. ASC-EVs fluorescence mean intensity was analysed for each antibody and compared to the controls following manufacturer's instruction.

Transmission Electron Microscopy

Purified EV samples were analyzed as previously described placed on 200 mesh nickel formvar carbon-coated grids (Electron Microscopy Science, Hatfield, Pennsylvania, USA) and left to adhere for 20 min. Next, grids were incubated with 2.5% glutaraldehyde containing 2% sucrose for 10 min and extensively washed in distilled water. Samples were than negatively stained with NanoVan (Nanoprobes, Yaphank, New York, USA) and analyzed using a Jeol JEM 1010 electron microscope (Jeol, Tokyo, Japan)[17].

NRG1 ELISA assay

ELISA assay was performed on protein derived from different ASC-EV preparations. Briefly, 100µl of ASC-EV proteins were loaded in a microtiter plate provided by NRG-1 ELISA kit (mybiosource) that has been coated with an anti-NRG-1 specific antibody. Details are reported in the *online Data Supplement.*

Molecular characterization of ASC-EV cargo

ASC-EV proteins from different preparations (n=8) were extracted using a lysis buffer provided by the Human L1000 (Glass Slide) protein array kit (Ray biotech). This kit allows the detection of 1,000 different proteins, including cytokines, chemokines, adipokines, growth factors, angiogenic factors, proteases, soluble receptors, adhesion molecules and other proteins to be simultaneously investigated.
Approximately 25 µg of protein were loaded for each sample. The fluorescence signal was subjected to background subtraction and the cut-off threshold was set as > 150 Fluorescence Intensity AU.

A PCR angiogenesis array was performed on total RNA that had been extracted from ASC-EVs (n=7) using a miRVANA isolation kit and quantified using a NanoDrop1000 spectrophotometer. The RT^2 First Strand kit (SABiosciences) was employed for cDNA synthesis, according to manufacturer's instructions. Two hundred ng of cDNA was run on an Angiogenesis RT^2 Profiler PCR Array (PAHS 024, PAMM-099Z, Qiagen, Frederick, MD, USA) to profile 84 key genes involved in angiogenesis (list of genes available on website: http://www.sabiosciences.com).
Data from the protein and mRNA arrays were compared and pathway enrichment analysis was performed using Funrich 3.1.3[18]. Data were considered significant at $p<0.05$ (Hypergeometric test with Bonferroni correction). Interaction network on selected proteins/genes was built using STRING online software. Details are reported in the *online Data Supplement.*

Cell culture

C2C12 cells (C2C12) were purchased from ATCC and cultured in DMEM high glucose (4.5 g/L-Lonza, Basel, Switzerland) and 20% FBS (Lonza). HMEC-1 (HMECs) were purchased from ATCC and cultured in Endothelial basal medium (EBM) (Lonza) and 10% FBS. SCs were isolated from the gastrocnemius muscles of C57BL/6J wild type mice subjected to ischemia. In order to obtain SCs, muscle samples were subjected to enzymatic digestion, as previously described[15].

In vitro assays

In vitro hypoxia model. The following *in vitro* model was used to simulate ischemia/reoxygenation (I/R) injury *in vitro*: cells (C2C12, differentiated myoblasts or HMECs) were cultured in a hypoxic gas mixture (1% O_2) for 8 hours in normal culture medium both with and without FBS. After hypoxia, cells were cultured in normoxic conditions, both with and without ASC-EVs (10,000 EVs/target cell), for 16 hours and then

analyzed for proliferation, apoptosis, RNA and protein expression for 6 days, for the differentiation experiments as described below.

Myoblast differentiation into myotubes: C2C12 were cultured in DMEM high glucose (4.5 g/L-Lonza, Basel, Switzerland) and 20% FBS (Lonza). When cells reached 80% confluence, cells were cultured in high glucose ± plus 2% horse serum DMEM for 6 days. In selected experiments, C2C12 were cultured in hypoxic gas mixture (1% O_2) for 8 hours and then cultured in normoxic conditions, both with and without 2% horse serum and ASC-EVs, for 6 days.

Proliferation: C2C12 and HMEC proliferation was performed via 5-bromo-2-deoxyuridine (BrdU) (Roche Diagnostics, Mannheim, Germany) incorporation in cells cultured in hypoxic conditions and incubated both with and without ASC-EVs. Details are reported in the *online Data Supplement.*

Apoptosis analysis in myoblasts and myotubes: C2C12 apoptosis was analysed using MUSE CELL Analyzer (Millipore), and a double staining with Annexin V and 7AAD. Briefly, cells were plated in 6 well plates, cultured in hypoxic gas mixture (1% O_2) for 8 hours and then cultured in normoxic conditions, both with and without ASC-EVs, for 16 hours and then analyzed. Myotube apoptosis was evaluated by counting the fragmented nuclei stained with Hoechst staining. Briefly, differentiated C2C12, plated in 6 well plates, were cultured in hypoxic gas mixture (1% O_2) for 8 hours and then cultured in normoxic conditions, both with and without ASC-EVs, for 16 hours. Normal and fragmented nuclei were counted in microphotographs that were obtained using a fluorescence microscope, and the percentage of apoptotic cells was calculate as the ratio between the number of fragmented nuclei and the number of total nuclei per microscopic field. In selected experiments ASC-EVs pretreated with a blocking NRG1 antibody, trypsin (0.25% w/v) and rhNRG1 (45 pg equivalent to $1.5x10^9$ ASC-EVs/$1.5x10^5$ cells) were used. Details are reported in the *online Data Supplement.*

RT-PCR array analysis

The Skeletal Muscle Myogenesis and Myopathy RT^2 Profiler PCR Array (PAMM-099Z, Qiagen) was used to characterize the gene expression profiles of the healthy and ischemic gastrocnemius muscles of C57BL/6J, both those treated with ASC-EVs and those untreated.

Briefly, according to manufacturer's instructions, RNA extracted from mouse muscles using the miRVANA kit was treated with gDNA elimination buffer to degrade DNA contamination, and then reverse-transcripted using RT^2 First Strand kit. Data analysis was performed using the RT^2Profiler PCR Array Data Analysis tool provided by the manufacturer (SABioscience). The expression levels of each gene were normalized for housekeeping genes. according to manufacturer's instructions. Details are reported in the *online Data Supplement.*

Real Time PCR analysis

The total RNA from the ischemic gastrocnemius muscles of C57BL/6J and hypoxic C2C12 (both those treated with ASC-EVs and those untreated, Different primers for mouse MyoD, Myogenin, Myf5, Pax7, p21 and p27 (*online Data Supplement* Table I) were used. Data analysis was performed using ExpressionSuite software (Life Technologies). In selected experiments the early growth response 1 (EGR1) gene was evaluated. The primer sequences are reported in *online Data Supplement*, Table I. Details are reported in the *online Data Supplement***.**

Western Blot

ASC-EVs, C2C12 and SCs were lysed in lysis buffer (RIPA buffer with proteinase inhibitors, Sigma Aldrich) for 1 hour at 4°C and centrifuged at 10,000 rcf. The supernatants were collected, quantified using the Bradford method and analyzed by western blot. The following primary antibodies were used: NRG1 (Raybiotech), CD63, MyoD, myogenin, CdK6, pho-p38MAPK, p38MAPK, Cyclin D1, p-Bcl-2, Bcl-XL, β-actin and vinculin (Santa Cruz). Densitrometric analysis was performed by Image Lab™ Software (BioRad) and data were expressed as arbitrary unit ± SD. Details are reported in the *online Data Supplement*.

Statistical analysis

Between-group comparisons were carried out by *t* test. Our data passed normality and equal variance tests. Comparisons between 3 or more groups were performed by one way ANOVA, and significance was evaluated using the Newman-Keuls multi-comparison *post hoc* test. The cut-off for statistical significance was set at $p < 0.05$. All statistical analyses were carried out on Graph Pad Prism version 5.04 (Graph Pad Software, Inc, USA).

RESULTS

Characterization of ASC-EVs

ASC-EVs were analyzed for their surface markers using Guava FACS analysis (*online Data Supplement* Figure 1). ASC-EV modal particle size corresponds to 160 nm (*online Data Supplement* Figure IA). No significant differences in ASC-EV number and size were observed over the various batches by Nanosight analyses. ASCs produced 11,411±2,316 EVs per cell, after overnight starvation. Detailed information to estimate EV number is reported in *online Data Supplement*. Starting from $2.25x10^{11}$ of total particles, the recovery of RNA and protein was similar in all the samples analyzed (n=21); about 275 ± 31 ng of RNA and about 30.52 ± 2.27 µg of protein. CD63, CD81 and CD9 exosomal marker expression was also detected using the MACSPlex kit for GUAVA FACS analysis (*online Data Supplement* Figure IB). Moreover, ASC-EVs showed the expression of CD29, CD44 and CD105 (ASC markers) and HLA I (*online Data Supplement* Figure IB). TEM was also performed and reported in *online Data Supplement* Figure 1C.

ASC-EVs prevent muscle damage in a mouse model of HLI

Preliminary experiments to identify the best administration route were performed by comparing two different administration routes as indicated in Materials and Methods section. Route 1: $1x10^{10}$ administrated intravenously immediately after intervention (T0), $0.5x10^{10}$ via intramuscular administration on day 1 (T1), and again on day 2 (T2); route 2: EVs were administered intramuscularly with the same timing and doses (T0:$1x10^{10}$; T1:$0.5x10^{10}$; T2:$0.5x10^{10}$) (*online Data Supplement* Figure 2). Therefore, to evaluate ASC-EV protection, mice that were subjected to the acute ischemic hind limb process were treated with $2x10^{10}$ ASC-EVs using the best administration route which corresponded to the route 1. The same volume of saline served as control. Blood perfusion of the ischemic hind limb, analyzed immediately after surgery by Laser Doppler, showed a strong reduction in blood flow (0.13±0.07 control group; 0.09±0.03 in ASC-EV group) (*online Data Supplement* Figure 3). Although no significant differences in large vessel reperfusion were found in the treatment groups, the saline group showed significantly higher functional damage scores than the ASC-EV-treated group (Figure 1A). In order to evaluate whether functional differences were a result of improvement in tissue reperfusion, vessel number was tallied in the ischemic muscles of treated animals at different time intervals (day 3 and 7); ASC-EV-treated animals showed a higher number of vessels than the saline group on day 7 quantified as number of small capillaries per number of muscle fiber (Figure 1B, D and *online Data Supplement Figure 4*). No differences were obtained counting large vessels (not shown). Furthermore, an analysis of gastrocnemius muscles revealed the presence of focal areas of damage in the saline group,. This effect was almost completely prevented by ASC-EV treatment (Figure 1C, D). These results suggest that, in our model, ASC-EV treatment protects muscles against ischemia-induced damage.

Gene array analysis of muscles from ASC-EV-treated animals

To investigate the ASC-EV mechanism of action muscles recovered on day 3 after surgery were analysed using a skeletal muscle specific gene array. As shown in Table 1/ *online Data Supplement* Table I and Figure 2A, ASC-EV treatment induced the expression of genes, such as MyoD, Myf5 and Pax7, that are involved in muscle cell proliferation, regeneration and differentiation. Primary SCs, recovered from healthy muscles, were also subjected to *in vitro* I/R and treated or not with ASC-EVs to further validate these data. As shown in Figure 2B, the ASC-EVs induced the expression of MyoD. As expected, myogenin did not change upon ASC-EV treatment (Figure 2A-B)

ASC-EVs induce myoblast proliferation

In order to validate the above data, the effect of ASC-EVs on myoblast proliferation was evaluated *using* murine myoblasts subjected to *in vitro* I/R. Based on our preliminary experiments using a variety of ASC-EV doses (data not shown), we decided to use 10000 EVs/target cell to evaluate ASC-EV biological effects. Fetal bovine serum treatment served as a positive control throughout the study. The proliferative effect of ASC-EVs on myoblasts that were subjected to treatment was evaluated. As shown in Figure 2C, ASC-EVs were able to induce myoblast proliferation in hypoxic conditions. Accordingly, cyclin D1 and CDK6 increased in myoblasts challenged with ASC-EVs (Figure 2D). The fact that myoblasts enter the cell-cycle is also supported by p38/MAPK activation (Figure 2D). These results were further validated by an analysis of the expression of cyclin kinase inhibitory genes, p21 and p27 (Figure 2E).

ASC-EVs induce myoblast differentiation and prevent apoptosis of both myoblasts and their differentiated counterparts

The effect of ASC-EVs on myoblast differentiation was also evaluated *in vitro* in murine myoblasts subjected to I/R. Data reported in Figure 3A, demonstrate that ASC-EV-treated myoblasts displayed a higher fusion index than untreated myoblasts. Moreover, the possibility that ASC-EVs may prevent apoptosis was also investigated. A double-staining, using annexin V and 7AAD, was performed. As shown in Figure 3B, ASC-EVs were able to increase the number of living cells and to reduce the number of apoptotic myoblasts. The expression of Bcl-XL and the phosphorylation of Bcl-2 were analysed for validation purposes. As reported in Figure 3C, ASC-EV treatment was associated with the increased expression of Bcl-XL and the phosphorylation of Bcl-2[19]. The anti-apoptotic effect of ASC-EVs was also evaluated in differentiated myoblasts by analyzing the morphological alterations that occur in nuclei in the final stages of apoptosis. Data reported in Figure 3D indicate that ASC-EV treatment decreased the percentage of fragmented nuclei in differentiated myoblasts. Unlike proliferation (PCNA) (*online Data Supplement* Figure 5), that occurs rapidly after I/R damage, we were able to demonstrate the anti-apoptotic effects of ASC-EVs *in vivo* (Figure 3E). These data indicate that ASC-EVs can protect muscles from I/R-induced damage by inducing myoblast proliferation, differentiation and by preventing apoptosis.

ASC-EV cargo drives proangiogenic and skeletal muscle protection mainly via NRG1-mediated signals

ASC-EVs were analyzed for their protein content. In particular, a protein array slide for the detection of cytokines, chemokines, adipokines, growth factors, angiogenic factors, proteases, soluble receptors and soluble adhesion molecules was used. As shown in *online Data Supplement* Table II, 237 proteins were detected in ASC-EVs. The most abundant proteins are reported in Table 2.

It is interesting to note that ASC-EVs were found to be enriched in NRG1 (Table 2, Figure 4A). ELISA assay demonstrated that $1X10^{10}$ ASC-EVs contain 300±7.07 pg of NRG1. NRG1 acts by binding to the ERBB tyrosine kinase receptors which activate a cascade of signaling pathways, including the p38MAPK pathway[20]. NRG1 controls both the proliferative and myogenic processes in skeletal muscle cells[21], while it drives endothelial cell proliferation in response to ischemia[22]. A blocking antibody against NRG1 was used to evaluate NRG1's contribution to ASC-EV-mediated protection. To this end, the BrdU assay and the expression of p38MAPK, cyclin D1 or p-Bcl-2 and Bcl-XL were evaluated in myoblasts subjected to ASC-EV treatment. As shown in Figure 4B-D, the NRG1 blockade prevented

ASC-EV-mediated myoblast proliferation and the transcription of EGR1, the NRG1 early response gene[23], while it was ineffective in preventing protection against I/R induced apoptosis (Figure 4E). rhNRG1 served as positive internal control. Moreover, the effect of the NRG1 blockade was also evaluated in endothelial cells subjected to ischemia as the involvement of NRG1 in endothelial cell proliferation has already been reported[24]. The results described in Figure 4F clearly demonstrate that ASC-EV-mediated endothelial cell proliferation and EGR1 transcription (*online Data Supplement* Figure 6) were inhibited by the NGR1 blockade. Finally, the pre-treatment of ASC-EVs with trypsin demonstrates that ASC-EV-mediated biological effects rely on having NRG1 bound to their membrane (Figure 4C and F).

NRG1 blockade prevent ASC-EV action *in vivo*

To further validate the above data, ASC-EVs pretreated with the anti-NRG1 blocking antibody were used for the *in vivo* study. As shown in Figure 5A-C the NRG1 blockade abrogates the ASC-EV pro-angiogenic effects as well as their protection against muscle damage (Figure 5B-C). Moreover, muscle damage was also evaluated at day 7 using nitro-blue tetrazolium staining. As shown in Figure 5B and *Data Supplement* Figure 7, ASC-EV were able to significantly reduce the ischemic area, while NRG1 blockade completely abrogated their effect. Of note, we failed to detect muscle protection when rhNRG1 was used as purified factor (300 pg) (data not shown). It has been recently shown that ASC-EV, obtained from patients undergoing abdominal surgery, promote inflammation in a preclinical model of I/R[25]. Our data clearly demonstrated that ASC-EV treatment did not increase the number of inflammatory cells (shown by CD14 staining) in the ischemic muscles (Figure 5A and C). Moreover, consistent with the potential role of NRG1 in regulating the inflammatory response[26], we found that ASC-EVs pre-treated with the anti-NRG1 blocking antibody were no more effective in preventing the recruitment of inflammatory cells (Figure 5A and C) and in promoting neoangionesis (Figure 5B and C and *online Data Supplement* Figure ~~7~~ 8).

ASC-EV mRNA and protein cargo can co-operate to boost angiogenesis and muscle regeneration after I/R damage

In order to gain further insight into the ASC-EV mechanism of action, ASC-EV mRNA content was analyzed using an RT-PCR array for the detection of the genes involved in angiogenesis. It is worth noting that gene array analysis highlighted enrichments in fibronectin 1, MMP2, Angiopoietin, FGF2, VEGFA and FLT1 mRNA. Moreover, the well-known modulators of both angiogenesis and muscle regeneration, HGF, IGF1 and EGF mRNA, were also found to be highly expressed (Table 3). A comparison of mRNA and the protein microarray led to 18 molecules being commonly detected in ASC-EVs (Figure 6A-B). Pathway enrichment analysis demonstrated that they are mainly involved in VEGF, Sphingosine 1-phosphate, PDGF, EGF, HGF and uPAR mediated signaling pathways (Figure 6C). Moreover, the interaction graph shown in Figure 6D indicates that there is close interplay between these molecules, which sustains the idea that they cooperate to induce angiogenesis and muscle regeneration in our model.

DISCUSSION

CLI is a common feature of patients with peripheral artery disease[1,27]. Since current therapeutic options are still ineffective new therapeutic strategies with which to improve patient outcomes are required. Adult stem cells are emerging as a cell-based therapy[4]. Of the stem cells available, ASCs are an ideal source[5]. They are easy available, show low immunogenicity and high proliferative capability[5] and were found effective in preclinical models of muscle atrophy[28] and peripheral artery disease[29].

A number of evidence indicates that advantages may be provided by secretome derivatives of stem cells, including EVs[5], in regenerative medicine and in therapeutic angiogenesis[30]. Herein, we investigated whether ASC-EVs could become a therapeutic tool with which to improve angiogenesis in mice that recapitulate human CLI. We have demonstrated that ASC-EVs display pro-angiogenic effects *in vivo*, as shown by the number of capillary/muscle fiber and by the analysis of capillary density. We have also found that mice treated with ASC-EVs present a lower score for hind limb functional damage than mice treated with the vehicle alone. Accordingly, histological analyses have highlighted that mice subjected to ASC-EV treatment had a reduced percentage of apoptotic cells and muscle damage. After damage, SCs enter the cell cycle by activating p38MAPK and inducing the expression of MyoD in the daughter cells[11]. Transcriptomic analysis, performed to detect early molecular events, has demonstrated that ASC-EV treatment induced the expression of genes associated with myoblast proliferation and differentiation, such as MyoD, Pax7 and Myf5, on day 3 after surgery. In accordance with these results, SCs that were exposed to ASC-EVs in ischemic/reoxigenation conditions increased the expression of MyoD. We further validated these data *in vitro*. Indeed, it has been demonstrated that ASC-EV challenge leads to an increase in the number of BrdU positive myoblasts. Accordingly, cyclin D1, CDK6 and p-p38/MAPK expression increased. Along with the effect on myoblast proliferation, we have also been able to demonstrate that ASC-EVs induced myoblast differentiation and prevented apoptotic signals in both myoblasts and their differentiated counterparts. As a matter of fact, ASC-EVs were able to increase the expression of Bcl-XL and the phosphorylation of Bcl2[19] in myoblasts and reduce the number of fragmented nuclei in differentiated myoblasts. These results sustain the possibility that protection against apoptosis and induction of vessel formation may well be the most relevant mechanisms via which a fast muscle regeneration/protection occurs. In line with this hypothesis, we failed to detect an increased number of regenerating myofibers and a decreased number of apoptotic cells at day 7 in ASC-EV-treated animals.

mRNAs, miRNAs, proteins and bioactive lipids are all recognized as relevant mediators of EV biological action in different regenerative processes[7]. However, miRNAs are the most studied proangiogenic drivers of stem-cell derived EV activities. This is also true for ASC-EVs[31,32,33]. We have demonstrated herein that ASC-EVs are also enriched in mRNAs that encode for a number of angiogenic regulators. More importantly, proteomic analyses of ASC-EV cargo has indicated relevant enrichment in NRG1, which is a member of the epidermal growth factor family that is also produced by skeletal muscles[34,35]. NRG1 regulates muscle cell homeostasis, SC survival and many relevant biological processes in skeletal muscles[36]. It exerts its biological effects by binding to NRG1 receptors, including ErbB3 and ErbB4 and the co-receptors ErbB1 and ErbB2[35]. We herein report that ASC-EV-delivered NRG1 may be involved in muscle protection against I/R damage, as is consistent with previous observations that demonstrate the involvement of the NRG1/ErbB system in muscle regeneration[20]. As a matter of fact, *in vitro* NRG1 blockade prevented the activation of p-p38MAPK, the expression of cyclin D1 and the transcription of ERG1 in myoblasts treated with ASC-EVs and subjected to I/R. These biochemical events *in vitro* translated into

the inhibition of myoblast proliferation and *in vivo* in the prevention of ASC-EV-mediated protection, as also supported by tetrazolium-staining. On the other hand, an NRG1-independent mechanism seems to be associated with protection against I/R-induced apoptosis in response to ASC-EV treatment. The IL-21R/IL-21 axis has been shown to prevent apoptosis and/or favor cell survival in hypoxic conditions[37]. Indeed, ASC-EVs were also enriched in IL-21, suggesting that ASC-EV-treatment-associated apoptosis resistance may rely on the IL-21-mediated signaling pathway. Further studies are required to validate this hypothesis.

It has been reported that endothelial cells express both NRG-1 and its receptors[24], and Hedhli *et al*.[22] have more recently demonstrated that NRG1 of endothelial origin is a crucial mediator of both angiogenesis and arteriogenesis in a hind limb ischemia model. In a finding that is consistent with these results, we have demonstrated that, just like in myoblasts, ASC-EVs promote endothelial cell proliferation and ERG1 transcription in hypoxic conditions and that these effects rely on ASC-EV-membrane-bound NRG1.

The recruitment of inflammatory cells is necessary to promote vascular growth upon damage. However, it has been recently shown that ASC-EVs, obtained from patients undergoing abdominal surgery, increased the recruitment of inflammatory cells without protecting muscles against I/R damage[25]. Of note, improvement of blood perfusion, protection of muscles, and a reduced infiltration of inflammatory cells were observed in mice treated with ASC-EVs released in response to PDGF[25]. The increase of IL-10 and TGF-β1 secretion by the inflammatory cells has been suggested to play a role in PDGF-driven ASC-EV action. This suggests the possibility that immunomodulatory mechanisms may be activated by ASC-EVs, including those mediated by NRG1[26]. Nonetheless, possibly due to the enrichment of proangiogenic mediators, ASC-EVs could induce a compensatory vascular growth able to protect muscle from damage even in the presence of a reduced number of inflammatory cells.

The existence of a dual ASC-EV biological effect, made up of angiogenesis and a hasty muscle protection, is therefore sustained by our *in vivo* results. Moreover, pathway enrichment analysis and, more importantly, the interaction graph further support the notion that cooperation between the bioactive molecules carried by ASC-EVs sustain and boost biological effects in our preclinical I/R model. This co-operative activity may provide a further explanation as to NRG1's independent protection against apoptosis in myoblasts and their differentiated counterparts, as well as to the failure of 300 pg rhNRG1, corresponding to its ASC-EV content, to recapitulate ASC-EV therapeutic effects.

EV therapeutic approaches have been proposed to solve a number of concerns about stem cell-based therapy in a range of clinical settings[5]. Our data demonstrate that the off-the-shelf ASC secretome may be a useful therapeutic approach with which to improve vascular growth and to protect muscles from I/R-mediated damage. Moreover, we have also identified NRG1 as one of the most relevant mechanisms for ASC-EV biological activity. Effort should now be placed into investigations of the therapeutic potential that ASC-EVs show for the treatment of a variety of pathological conditions in which muscle protection is required.

Limitations

We are confident that the intrinsic curb of Laser Doppler Perfusion analysis, prevents the detection of the profound vascular districts. However, histological analyses clearly demonstrated that, upon ASC-EV treatment, an increased n°capillary/n°muscle fiber are present in the ischemic muscles. Moreover, concerns could be also raised by the protocol

we adopted, owing to the minimal residual blood flow (10%) detected after surgery (see *online Data Supplement*, Figure 3). However, based on our results, it can be speculated that i.v. ASC-EVs administration at T0, may have dual beneficial effects: locally, to boost of a hasty angiogenic response, systemically, to activate signals in circulating inflammatory cells impairing their recruitment into ischemic tissues, and prevent damage. Finally, since a low residual blood flow is a common feature in CLI patients undergoing revascularization, it could be speculated that this protocol might be beneficial even in clinical settings.

ACKNOWLEDGMENTS none

SOURCES OF FOUNDING This work was supported by grant No. 071215 from Unicyte to 2i3T to GC and MFB. Associazione Italiana per la Ricerca sul Cancro (AIRC) project IG 2015.17630 to MFB.

DISCLOSURES

G.C. is a component of Scientific Advisory Board of Unicyte AG.

REFERENCES

1. Olin JW, White CJ, Armstrong EJ, Kadian-Dodov D, Hiatt WR. Peripheral Artery Disease. *N Engl J Med*. 2016; 67(5):558-587.
2. Vartanian SM, Conte MS. Surgical Intervention for Peripheral Arterial Disease. *Circ Res*. 2015;116(9):1614-1628.
3. Thukkani AK, Kinlay S, Hospital MB, Divisions C. Endovascular intervention for peripheral artery disease. *Circ Res*. 2015;116 (9):1599-1613.
4. Gupta NK, Armstrong EJ, Parikh SA. The current state of stem cell therapy for peripheral artery disease. *Curr Cardiol Rep*. 2014;16 (2):447.
5. Vizoso FJ, Eiro N, Cid S, Schneider J, Perez-Fernandez R. Mesenchymal stem cell secretome: Toward cell-free therapeutic strategies in regenerative medicine. *Int J Mol Sci*. 2017;18(9):E1852.
6. Bronckaers A, Hilkens P, Martens W, Gervois P, Ratajczak J, Struys T, Lambrichts I. Mesenchymal stem/stromal cells as a pharmacological and therapeutic approach to accelerate angiogenesis. *Pharmacol Ther*. 2014;143(2):181-196.
7. Camussi G. Stem Cell Reviews and Reports: Microenvironment and Extracellular Microvesicles Section. *Stem Cell Rev Reports*. 2017;13(1):4.
8. Lee Y, El Andaloussi S, Wood MJA. Exosomes and microvesicles: Extracellular vesicles for genetic information transfer and gene therapy. *Hum Mol Genet*. 2012; 21(R1):R125-R134.
9. Liu L, Jin X, Hu CF, Li R, Zhou Z, Shen CX. Exosomes Derived from Mesenchymal Stem Cells Rescue Myocardial Ischaemia/Reperfusion Injury by Inducing Cardiomyocyte Autophagy Via AMPK and Akt Pathways. *Cell Physiol Biochem*. 2017;43(1):52-68.
10. Herrera MB, Fonsato V, Gatti S, Deregibus MC, Sordi A, Cantarella D, Calogero R, Bussolati B, Tetta C, Camussi G. Human liver stem cell-derived microvesicles accelerate hepatic regeneration in hepatectomized rats. *J Cell Mol Med*. 2010. 14(6B):1605-1618.
11. Jones NC, Tyner KJ, Nibarger L, Stanley HM, Cornelison DDW, Fedorov Y V., Olwin BB. The p38α/β MAPK functions as a molecular switch to activate the quiescent satellite cell. *J Cell Biol*. 2005;169(1):105-116.
12. Zhao L, Johnson T, Liu D. Therapeutic angiogenesis of adipose-derived stem cells for ischemic diseases. *Stem Cell Res Ther*. 2017;8(1):125.
13. Cavallari C, Ranghino A, Tapparo M, Cedrino M, Figliolini F, Grange C, Giannachi V, Garneri P, Deregibus MC, Collino F, Rispoli P, Camussi G, Brizzi MF. Serum-derived extracellular vesicles (EVs) impact on vascular remodeling and prevent muscle damage in acute hind limb ischemia. *Sci Rep*. 2017;7(1):8180.
14. Ranghino A, Cantaluppi V, Grange C, Vitillo L, Fop F, Biancone L, Deregibus MC, Tetta C, Segoloni GP, Camussi G. Endothelial progenitor cell-derived microvesicles improve neovascularization in a murine model of hindlimb ischemia. *Int J Immunopathol Pharmacol*. 2012;25(1):75-85.
15. Togliatto G, Trombetta A, Dentelli P, Cotogni P, Rosso A, Tschöp MH, Granata R, Ghigo E, Brizzi MF. Unacylated ghrelin promotes skeletal muscle regeneration following hindlimb ischemia via SOD-2-mediated miR-221/222 expression. *J Am Heart Assoc*. 2013;2(6):e000376.
16. Penna C, Tullio F, Femminò S, Rocca C, Angelone T, Cerra MC, Gallo MP, Gesmundo I, Fanciulli A, Brizzi MF, Pagliaro P, Alloatti G, Granata R. Obestatin regulates cardiovascular function and promotes cardioprotection through the nitric oxide pathway. *J Cell Mol Med*. 2017;21(12):3670-3678.
17. Deregibus MC, Figliolini F, D'Antico S, Manzini PM, Pasquino C, De Lena M, Tetta

C, Brizzi MF, Camussi G. Charge-based precipitation of extracellular vesicles. *Int J Mol Med*. 2016;38(5):1359-1366.
18. Benito-Martin A, Peinado H. FunRich proteomics software analysis, let the fun begin! *Proteomics*. 2015;15(15):2555-2556.
19. Campbell TL, Mitchell AS, McMillan EM, Bloemberg D, Pavlov D, Messa I, Mielke JG, Quadrilatero J. High-fat feeding does not induce an autophagic or apoptotic phenotype in female rat skeletal muscle. *Exp Biol Med*. 2015;240(5):657-668.
20. Hirata M, Sakuma K, Okajima S, Fujiwara H, Inashima S, Yasuhara M, Kubo T. Increased expression of neuregulin-1 in differentiating muscle satellite cells and in motoneurons during muscle regeneration. *Acta Neuropathol*. 2007;113(4):451-459.
21. Ho AT Van, Hayashi S, Bröhl D, Auradé F, Rattenbach R, Relaix F. Neural Crest Cell Lineage Restricts Skeletal Muscle Progenitor Cell Differentiation through Neuregulin1-ErbB3 Signaling. *Dev Cell*. 2011;21(2):273-287.
22. Hedhli N, Dobrucki LW, Kalinowski A, Zhuang ZW, Wu X, Russell RR, Sinusas AJ, Russell KS. Endothelial-derived neuregulin is an important mediator of ischaemia-induced angiogenesis and arteriogenesis. *Cardiovasc Res*. 2012;93(3):516-524.
23. Jacobson C, Duggan D, Fischbach G. Neuregulin induces the expression of transcription factors and myosin heavy chains typical of muscle spindles in cultured human muscle. *Proc Natl Acad Sci*. 2004;101(33):12218-12223.
24. Russell KS, Stern DF, Polverini PJ, Bender JR. Neuregulin activation of ErbB receptors in vascular endothelium leads to angiogenesis. *Am J Physiol*. 1999;277(6):H2205-H2211.
25. Lopatina T, Favaro E, Grange C, Cedrino M, Ranghino A, Occhipinti S, Fallo S, Buffolo F, Gaykalova DA, Zanone MM, Romagnoli R, Camussi G. PDGF enhances the protective effect of adipose stem cell-derived extracellular vesicles in a model of acute hindlimb ischemia. *Sci Rep*. 2018;8(1):17458.
26. Ryzhov S, Matafonov A, Galindo CL, Zhang Q, Tran T-L, Lenihan DJ, Lenneman CG, Feoktistov I, Sawyer DB. ERBB signaling attenuates proinflammatory activation of nonclassical monocytes. *Am J Physiol Circ Physiol*. 2017;312(5):H907-H918.
27. Krishna SM, Moxon J V., Golledge J. A review of the pathophysiology and potential biomarkers for peripheral artery disease. *Int J Mol Sci*. 2015;16(5):11294-11322.
28. Park JU, Kwon ST. Potential of autologous adipose-derived stem cells to regenerate atrophied muscle in a rat model. *Wound Repair Regen*. 2017;25(6):944-955.
29. Rybalko V, Hsieh PL, Ricles LM, Chung E, Farrar RP, Suggs LJ. Therapeutic potential of adipose-derived stem cells and macrophages for ischemic skeletal muscle repair. *Regen Med*. 2017;12(2):153-167.
30. Camussi G, Deregibus MC,Quesenberry PJ. Role of Stem Cell-derived Extracellular RNA-carrying Vesicles Cell Reprogramming *Austin J Clin Pathol*. 2014;1(1):1001.
31. Kang T, Jones TM, Naddell C, Bacanamwo M, Calvert JW, Thompson WE, Bond VC, Chen YE, Liu D. Adipose-Derived Stem Cells Induce Angiogenesis via Microvesicle Transport of miRNA-31. *Stem Cells Transl Med*. 2016;5(4):440-450.
32. Lopatina T, Bruno S, Tetta C, Kalinina N, Porta M, Camussi G. Platelet-derived growth factor regulates the secretion of extracellular vesicles by adipose mesenchymal stem cells and enhances their angiogenic potential. *Cell Commun Signal*. 2014;12:26.
33. Togliatto G, Dentelli P, Gili M, Gallo S, Deregibus C, Biglieri E, Iavello A, Santini E, Rossi C, Solini A, Camussi G, Brizzi MF. Obesity reduces the pro-angiogenic potential of adipose tissue stem cell-derived extracellular vesicles (EVs) by impairing miR-126 content: Impact on clinical applications. *Int J Obes*. 2016;40(1):102-111.
34. Meyer D, Yamaai T, Garratt A, Riethmacher-Sonnenberg E, Kane D, Theill LE, Birchmeier C. Isoform-specific expression and function of neuregulin. *Development*.

1997;124(18):3575-3586.
35. Britsch S. The neuregulin-I/ErbB signaling system in development and disease. *Adv Anat Embryol Cell Biol*. 2007;190:1-65.
36. Guma A, Martinez-Redondo V, Lopez-Soldado I, Canto C, Zorzano A. Emerging role of neuregulin as a modulator of muscle metabolism. *AJP Endocrinol Metab*. 2010;298(4):E742-E750.
37. Wang T, Cunningham A, Dokun AO, Hazarika S, Houston K, Chen L, Lye RJ, Spolski R, Leonard WJ, Annex BH. Loss of interleukin-21 receptor activation in hypoxic endothelial cells impairs perfusion recovery after hindlimb ischemia. *Arterioscler Thromb Vasc Biol*. 2015;35(5):1218-1225.

HIGHLIGHTS

- ASC-EVs prevent muscle damage after acute hind limb ischemia
- ASC-EVs induce vascular growth and protect muscle against I/R damage
- ASCs-EVs are enriched in NRG1 and pro-angiogenic mRNAs
- ASC-EVs via NRG1 impair inflammatory cell infiltration in muscles subjected to I/R

FIGURE LEGENDS

Figure 1. Effects of ASC-EVs on I/R damage. **A,** Foot damage score on different days (0, 1, 3, 7) after surgery in ASC-EV treated and untreated mice. Data are expressed as mean ± SD; *p value < 0.05 ASC-EVs vs Vehicle, (One way Anova - Newman-Keuls Multiple Comparison Test), (n=8). **B,** Quantitative analysis of the capillary density of normal and ischemic hind limbs on days 3 and 7 after surgery. Data are expressed as mean ± SEM n°capillaries/n°of muscle fiber; *p value < 0.05, ASC-EVs vs Vehicle, (One-Way Anova - Newman-Keuls Multiple Comparison Test) (n=8). **C,** Quantitative analysis of muscle damage areas in hematoxylin-eosin stained gastrocnemius muscles of normal and ischemic hind limbs on days 3 and 7 after surgery. Data are expressed as percentage of damage area ± SEM; *p value < 0.05 ASC-EVs vs Vehicle, (One way Anova - Newman-Keuls Multiple Comparison Test) (n=8). **D**, Representative hematoxylin-eosin and Masson's trichrome images of non-ischemic (Normal) and ischemic hind limb gastrocnemius muscles in Vehicle- and ASC-EV-treated animals after 3 (3D) and 7 (7D) days post-surgery (Original Magnification: x200 for hematoxylin-eosin – scale bar: 50μm and x400 – scale bar: 25μm for Masson's trichrome). Arrows indicate the capillaries.

Figure 2. ASC-EVs induce the expression of differentiation genes in muscles and in satellite cells exposed to I/R and induce proliferation on myoblast in vitro. A, Total RNA from I/R gastrocnemius muscles, both treated (ASC-EVs) and untreated (C) were analyzed for the expression of muscle differentiation genes (MyoD, Myogenin, Myf5, Pax7) by RT-PCR. Results are expressed as relative quantification (RQ) of data normalized for housekeeping genes. The results are representative of 3 different experiments (n=3) (* p<0.05 ASC-EVs vs C for MyoD, Pax7; **p<0.01 ASC-EVs vs C for Myf5). **B,** SCs recovered from normo-perfused muscles were subjected to I/R. Cell extracts were analyzed for MyoD and Myogenin content by densitometry (Relative amount). Protein levels were normalized to β-actin content. The results are representative of 3 different experiments (n=3 * p<0.05 ASC-EVs vs C). **C,** Myoblasts were cultured in hypoxic conditions in medium with (C+) or without (C-) FBS, in the presence and in the absence of ASC-EVs (ASC-EVs), and evaluated for BrdU incorporation (n=3 *p<0.05 ASC-EVs vs C- ; **p<0.01 C+ vs C-). **D,** Representative images and relative densitometric analysis of CdK6, Cyclin D1 and p-p38MAPK protein expression in myoblasts treated as above and normalized for either β-actin or p38MAPK. The same blot was used to evaluate CdK6, Cyclin D1 and p-p38MAPK expression. Results are representative of all samples (n=3 *p<0.05 ASC-EVs vs C-). **E,** p21 and p27 RQ expression in myoblasts treated as above and normalized for the housekeeping gene (p21, p27: *p<0.05 ASC-EVs vs C-)

Figure 3. Effects of ASC-EVs on myoblast differentiation and apoptosis. A, After hypoxia, myoblasts were cultured in normoxic conditions in medium supplemented with 10% FBS (C-) either with 2% horse serum (differentiation condition) with ASC-EVs (ASC-EVs) or without ASC-EVs (C+) (*p<0.05 ASC-EVs vs C-). Fusion index was calculated by the ratio between the number nuclei detected in myotubes expressing the myosin heavy chain (nuclei > 2 was considered positive) and the total number of nuclei. **B,** Apoptosis assay on myoblasts cultured in hypoxic conditions in medium with (C+) or without (C-) FBS either in the presence (ASC EVs) or absence of ASC-EVs (*p<0.05 C+ and ASC-EVs vs C-). **C,** Representative images and relative densitometric analysis of p-Bcl-2 and Bcl-XL protein expression in myoblasts treated as above and normalized for vinculin. The same blot was used to evaluate p-Bcl-2 and Bcl-XL protein expression. Results are representative of all samples (n=5 *p< 0.05 ASC-EVs vs C-). **D,** Representative images and quantification of nuclei fragmentation in myotubes cultured in hypoxic conditions in the presence (C+) and

the absence (C-) of FBS, both with and without ASC-EVs (n=3 *p<0.05 ASC-EVs vs C-, **p<0.01 C + vs C-) (yellow arrows indicate apoptotic nuclei). **E,** Apoptosis in ischemic muscles was evaluated at day 7 after surgery upon ASC-EV (ASC-EVs) or saline treatment (C-). The expression of the percentage of apoptotic cells is reported (*p<0.05 ASC-EVs vs C-)

Figure 4. Role of NRG1 in ASC-EV-mediated myoblast and endothelial cell proliferation. A, Expression of NRG1, CD63 and vinculin in ASC-EVs, renal tubular (C-) and myotube cells (C+) were used as negative control and positive control respectively. **B,** BrdU analysis of myoblasts cultured in hypoxic conditions, with (C+) and without (C-) FBS, in the presence and in the absence of ASC-EVs (ASC-EVs), ASC-EVs treated with an anti-NRG1 blocking antibody (ASC-EVs + anti-NRG1) or with trypsin (ASC-EVs + trypsin) (n=3 **p<0.01 ASC-EVs vs C-; *p<0.05 ASC-EVs vs ASC-EVs + anti-NRG1 and ASC-EVs + trypsin). **C and E,** myoblasts cultured as above and evaluated for p-p38MAPK, Cyclin D1 **(C)**, p-Bcl-2 and Bcl-XL **(E)**. The same blot was used to evaluate p-p38MAPK, Cyclin D1, p-Bcl-2 and Bcl-XL protein expression. Densitometric analysis of C and E (Relative amount). Protein levels were normalized to p38/MAPK and/or vinculin. (n=3 *p<0.05 ***p<0.001). **D**, qRT-PCR analysis of ERG1 in myoblasts cultured in hypoxic condition for 1 hour, without FBS (C-), with rhNRG1, ASC-EVs (ASC-EVs) or ASC-EVs treated with an anti-NRG1 blocking antibody (ASC-EVs + anti-NRG1) (n=3 *p<0.05 C- vs NRG1, **p<0.01 C- vs ASC-EVs) is reported. **F,** BrdU incorporation in human endothelial cells (HMECs) cultured in hypoxic conditions in medium, with (C+) and without (C-) FBS, in the presence and in the absence of ASC-EVs (ASC-EVs), ASC-EVs treated with an anti-NRG1 blocking antibody (ASC-EVs + anti-NRG1) and with trypsin (ASC-EVs + trypsin) (n=3 *p<0.05 ASC-EVs vs C-; *p<0.05 ASC-EVs vs ASC-EVs + anti-NRG1 and ASC-EVs + trypsin).

Figure 5. ASC-EVs prevent the inflammatory response via NRG1

A, Representative immunofluorescence images of inflammation. Anti-CD14 mAb was used to analyze gastrocnemius muscles of ischemic hind limb in Vehicle, ASC-EVs- and ASC-EVs + anti-NRG1 treated animals as indicated (Original Magnification: X400 - scale bar: 25 μm). The negative control for primary antibodies is indicated as"-". **B,** Representative hematoxylin-eosin, Masson's trichrome, and NTB images of gastrocnemius muscles of ischemic hind limb in Vehicle, ASC-EVs and ASC-EVs plus anti-NRG1 treated animals (Original Magnification: x200 for hematoxylin-eosin – scale bar: 50μm and x400 – scale bar: 25μm for Masson's trichrome). Arrows indicate the capillaries and the ischemic area in the NTB sections. **C,** Quantitative analyses of capillaries (n°capillaries/n°muscle fiber), CD14+ cells and the percentage of the ischemic area in Vehicle, ASC-EV and ASC-EV ≠ plus anti-NRG1 ischemic hind limb at day 7 after surgery are reported. Data are expressed as mean ± SEM; *p value < 0.05, ASC-EVs vs Vehicle, (One-Way Anova - Newman-Keuls Multiple Comparison Test) (n=8 for quantification capillary density and CD14+ cells, and n=4 for NTB analysis).

Figure 6. **ASC–EV cargo characterization and pathway enrichment analysis. A,** Venn diagram showing the comparison between mRNAs and proteins carried by ASC-EVs. **B,** List of the 18 molecules carried by ASC-EVs, such as mRNAs and proteins. **C,** Biological pathways in which the 18 mRNA/proteins are mainly involved. Many enriched pathways are related to angiogenesis and muscle regeneration. Bioinformatic analysis was performed using Funrich V3 software. The blue bar represents the percentage of genes involved in the specific pathway; the red bar represents the significant p-value. (p<0.05 Hypergeometric test with Bonferroni test correction). **D,** Interaction graph analysed by String on line software showing relationship between the 18 identified proteins. Red arrows indicate inhibition; green arrows indicate activation; blue arrows indicate protein binding.

TABLE 1

Gene Symbol	Fold Regulation	SD
Myod1	3.85	± 0.30
Myf5	2.97	± 0.18
Il6	2.89	± 0.17
Cav1	2.33	± 0.50
Igf2	2.03	± 0.79
Ppargc1a	1.71	± 0.59
Ppargc1b	1.71	± 0.78
Igf1	1.69	± 0.49
Ctnnb1	1.69	± 0.67
Capn2	1.62	± 0.31
Capn3	1.62	± 0.51
Prkaa1	1.61	± 0.58
Lmna	1.58	± 0.24
Cs	1.57	± 0.81
Il1b	1.55	± 0.30
Agrn	1.55	± 0.61
Mapk14	1.53	± 0.75
Prkag1	1.52	± 0.80
Pax7	1.52	± 0.62
Ikbkb	0.65	± 0.21
Foxo1	0.59	± 0.15
Myh1	0.56	± 0.18
Tgfb1	0.54	± 0.25
Lep	0.24	± 0.19

Table 1. List of mRNAs modulated in ASC-EV-treated muscles, compared with untreated muscles. RQ (fold regulation) values are evaluated using: $2^{-\Delta\Delta Ct}$ ± SD (n=4).

TABLE 2

Protein	Gene Name	Fluorescence intensity	SD
Neuregulin 1	**NRG1**	50176	± 10353.11
LAG-3	**LAG3**	1979	± 184.91
Amylin	**IAPP**	753	± 144.60
IL-21	**IL21**	647	± 88.75
IL-13	**IL13**	632	± 80.76
GDF11	**GDF11**	626	± 129.04
HGFR	**MET**	625	± 123.97
MSHa	**MSX1**	590	± 43.49
GDF3	**GDF3**	587	± 78.70
Granzyme A	**GZMA**	573	± 13.92
BD-1	**DEFB1**	563	± 54.33
GDF5	**GDF5**	556	± 73.55
GDF9	**GDF9**	552	± 80.80
MIP-3 beta	**CCL19**	539	± 153.82
GRO	**CXCL2**	533	± 21.26
IFN-gamma	**IFNG**	530	± 34.57
GDF8	**MSTN**	527	± 51.67
IL-5	**IL5**	512	± 27.15

Table 2. List the most abundant proteins in ASC-EVs.

TABLE 3

Gene symbol	40 - Ct (± SD)	Gene symbol	40 - Ct (± SD)	Gene symbol	40 - Ct (± SD)
FN1	9.57 ± 0.79	**ANGPT1**	7.33 ± 0.53	**ANGPTL4**	6.63 ± 0.72
COL4A3	8.76 ± 0.68	**TIMP2**	7.29 ± 0.84	**ANG**	6.61 ± 0.49
PGF	8.76 ± 0.81	**IL6**	7.28 ± 0.87	**ENG**	6.55 ± 0.95
MMP2	8.49 ± 0.71	**TIMP1**	7.24 ± 2.1	**PTGS1**	6.49 ± 1.34
PLG	8.31 ± 0.68	**SERPINF1**	7.24 ± 1.11	**CCL2**	6.47 ± 0.54
HGF	8.31 ± 0.79	**AKT1**	7.21 ± 0.99	**VEGFC**	6.43 ± 1.11
IGF1	8.30 ± 0.71	**ANPEP**	7.21 ± 0.76	**EFNA1**	6.37 ± 0.91
TEK	8.24 ± 0.75	**EFNB2**	7.20 ± 0.51	**TNF**	6.29 ± 0.66
FGF2	8.19 ± 0.66	**CXCL6**	7.19 ± 0.85	**CTGF**	6.29 ± 0.50
HIF1A	7.98 ± 0.59	**HPSE**	7.09 ± 0.86	**NOS3**	6.13 ± 0.84
VEGFA	7.94 ± 0.73	**THBS1**	7.07 ± 1.10	**VEGFB**	6.12 ± 0.79
EDN1	7.93 ± 1.34	**EPHB4**	7.05 ± 0.57	**CXCL5**	6.10 ± 0.55
PF4	7.85 ± 0.64	**NRP1**	7.03 ± 0.81	**LECT1**	6.08 ± 1.08
CXCL9	7.78 ± 0.69	**THBS2**	7.02 ± 0.87	**CDH5**	5.97 ± 0.74
FGF1	7.77 ± 0.82	**CCL11**	7.01 ± 0.91	**LEP**	5.92 ± 0.73
TGFB2	7.73 ± 0.61	**TGFA**	6.94 ± 0.58	**ITGB3**	5.85 ± 0.91
ITGAV	7.71 ± 0.79	**TIE1**	6.92 ± 0.83	**MMP14**	5.78 ± 0.71
PROK2	7.69 ± 0.93	**TGFB1**	6.89 ± 0.72	**IL1B**	5.72 ± 0.76
EGF	7.6 ± 0.98	**COL18A1**	6.89 ± 0.61	**SPHK1**	5.57 ± 0.75
FLT1	7.57 ± 0.64	**PDGFA**	6.85 ± 0.59	**PLAU**	5.48 ± 0.73
IL8	7.55 ± 0.78	**KDR**	6.84 ± 0.38	**FGFR3**	5.38 ± 0.79
IFNG	7.51 ± 0.88	**F3**	6.83 ± 0.57	**ID1**	5.14 ± 0.81
IFNA1	7.50 ± 0.67	**TGFBR1**	6.81 ± 1.19	**S1PR1**	5.08 ± 0.83
SERPINE1	7.46 ± 0.75	**BAI1**	6.79 ± 0.70	**ERBB2**	5.03 ± 0.63
FIGF	7.45 ± 0.50	**NRP2**	6.78 ± 0.61	**PECAM1**	4.91 ± 0.46
TIMP3	7.42 ± 0.72	**ANGPT2**	6.75 ± 0.48	**NOTCH4**	4.80 ± 0.97
JAG1	7.39 ± 0.92	**MMP9**	6.71 ± 0.75	**TYMP**	4.51 ± 0.61
CXCL10	7.38 ± 1.06	**CXCL1**	6.68 ± 0.71	**MDK**	3.27 ± 0.65

Table 3. Complete list of mRNAs involved in angiogenesis analyzed in ASC-EVs. 40 - Ct values were calculated by subtracting the mean gene Ct from 40 total RT PCR cycles (±SD).

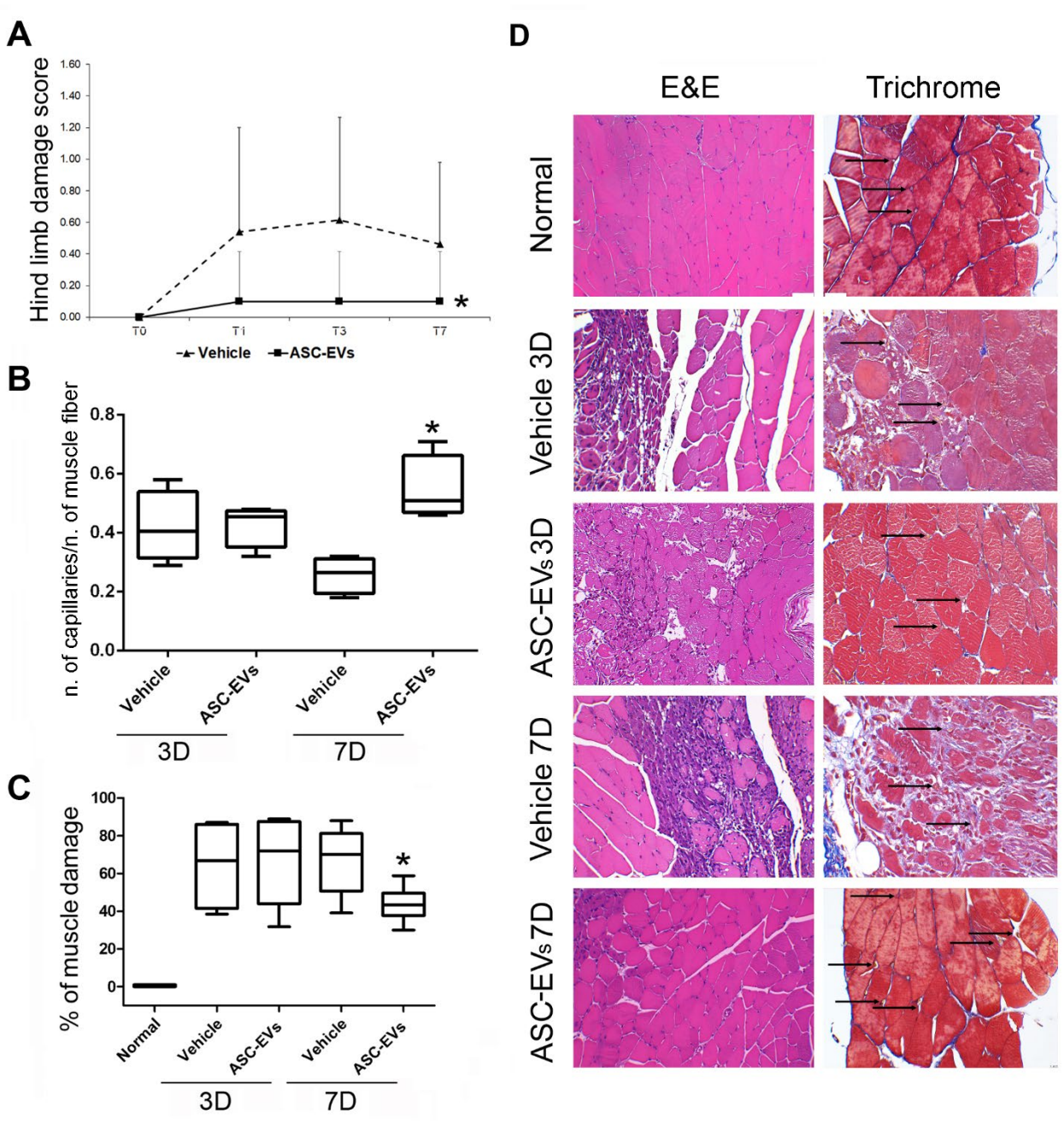
A
Hind limb damage score
1.60
1.40
1.20
1.00
0.80
0.60
0.40
0.20
0.00
T0
T1
T3
T7
*
Vehicle
ASC-EVs
B
n. of capillaries/n. of muscle fiber
0.8
0.6
0.4
0.2
0.0
*
Vehicle
ASC-EVs
Vehicle
ASC-EVs
3D
7D
C
% of muscle damage
100
80
60
40
20
0
*
Normal
Vehicle
ASC-EVs
Vehicle
ASC-EVs
3D
7D
D
E&E
Trichrome
Normal
Vehicle 3D
ASC-EVs 3D
Vehicle 7D
ASC-EVs 7D

Figure 1

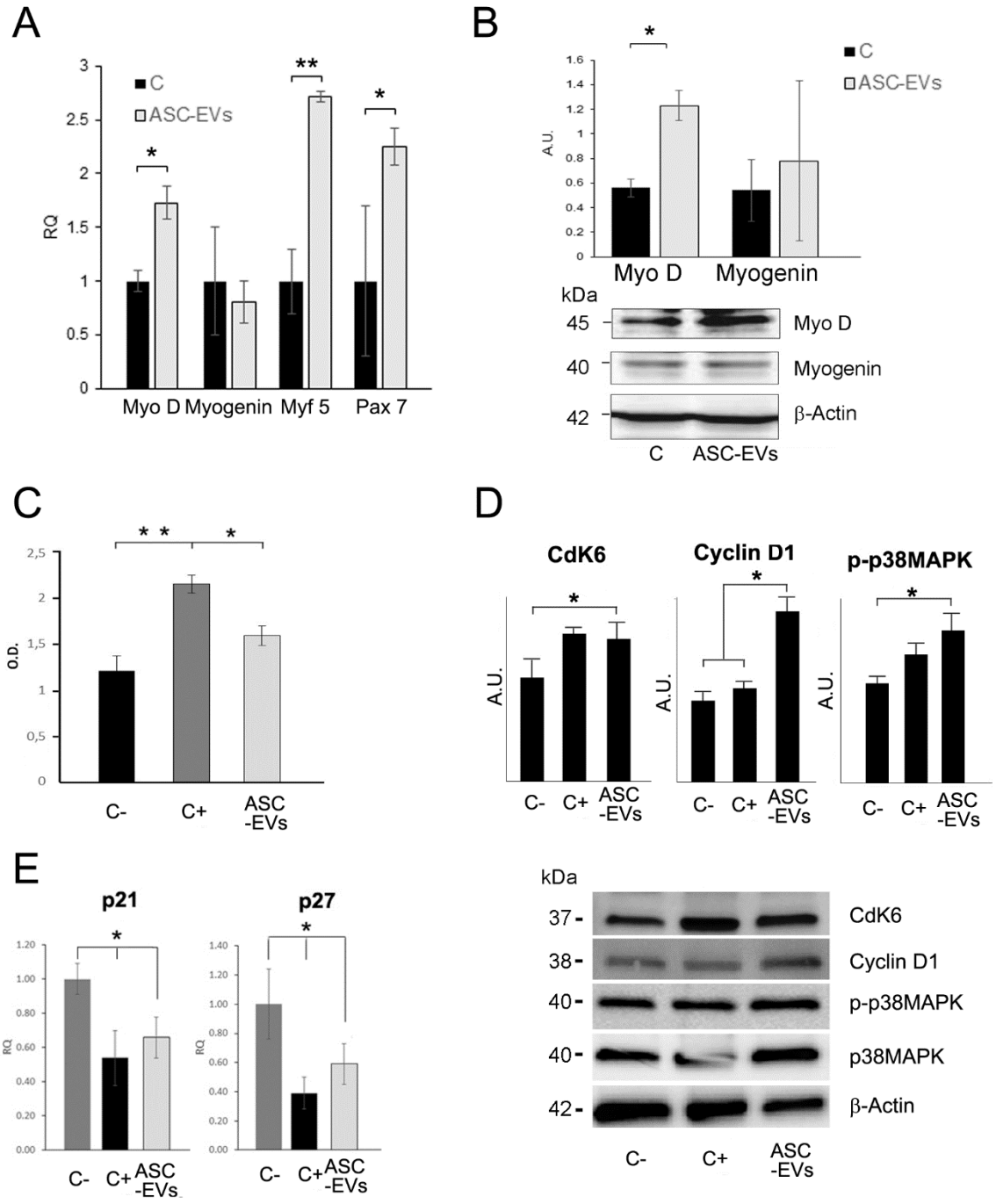
A
C
ASC-EVs
RQ
Myo D
Myogenin
Myf 5
Pax 7
B
C
ASC-EVs
A.U.
Myo D
Myogenin
kDa
45
40
42
Myo D
Myogenin
β-Actin
C
ASC-EVs
C
O.D.
C-
C+
ASC -EVs
D
CdK6
Cyclin D1
p-p38MAPK
A.U.
C-
C+
ASC -EVs
E
p21
p27
RQ
C-
C+
ASC -EVs
kDa
37
38
40
40
42
CdK6
Cyclin D1
p-p38MAPK
p38MAPK
β-Actin
C-
C+
ASC -EVs

Figure 2

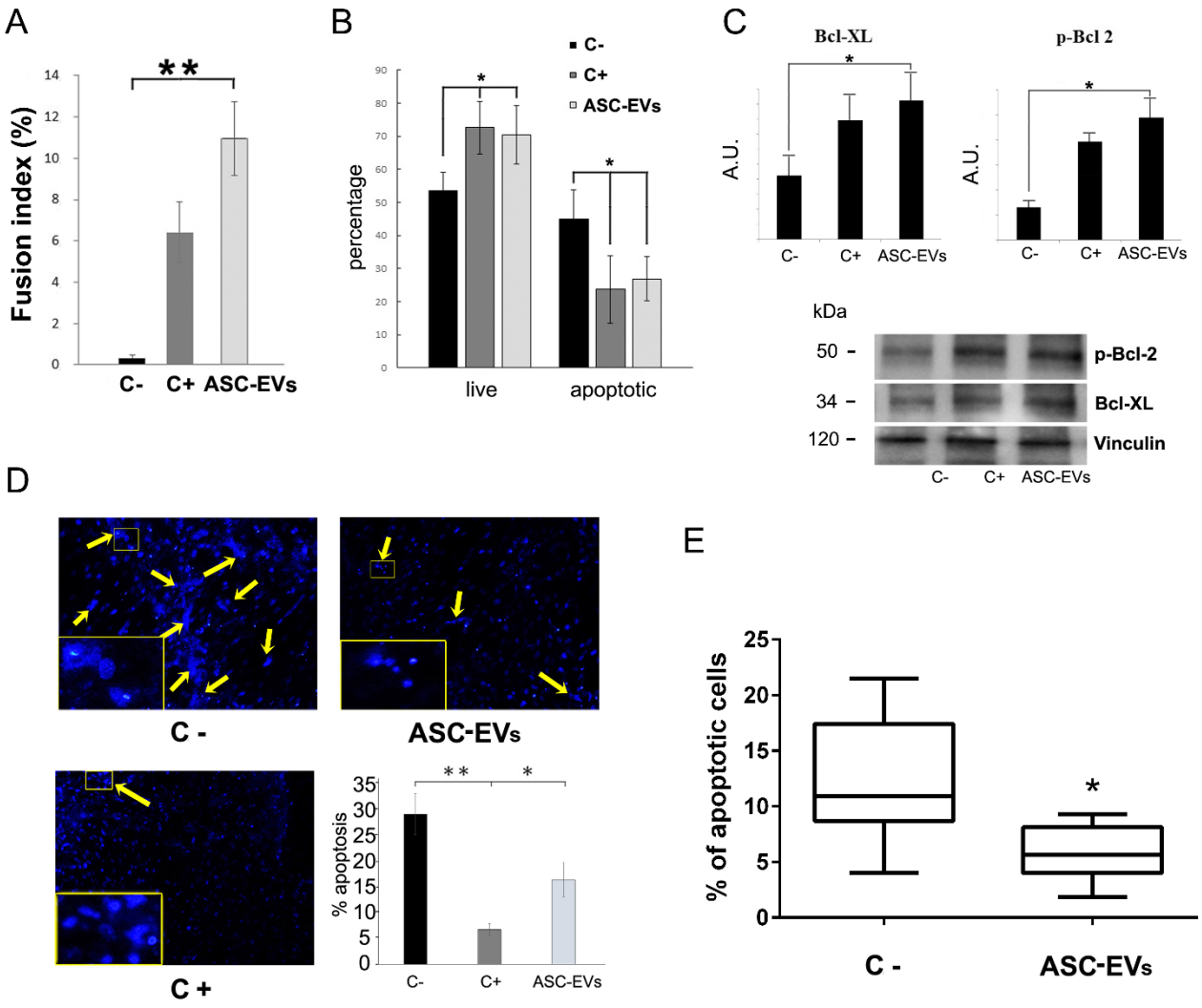
A
Fusion index (%)
**
C- C+ ASC-EVs
B
C-
C+
ASC-EVs
percentage
live
apoptotic
C
Bcl-XL
p-Bcl 2
A.U.
C- C+ ASC-EVs
kDa
50
34
120
p-Bcl-2
Bcl-XL
Vinculin
C- C+ ASC-EVs
D
C -
ASC-EVs
C +
% apoptosis
C- C+ ASC-EVs
E
% of apoptotic cells
C -
ASC-EVs

Figure 3

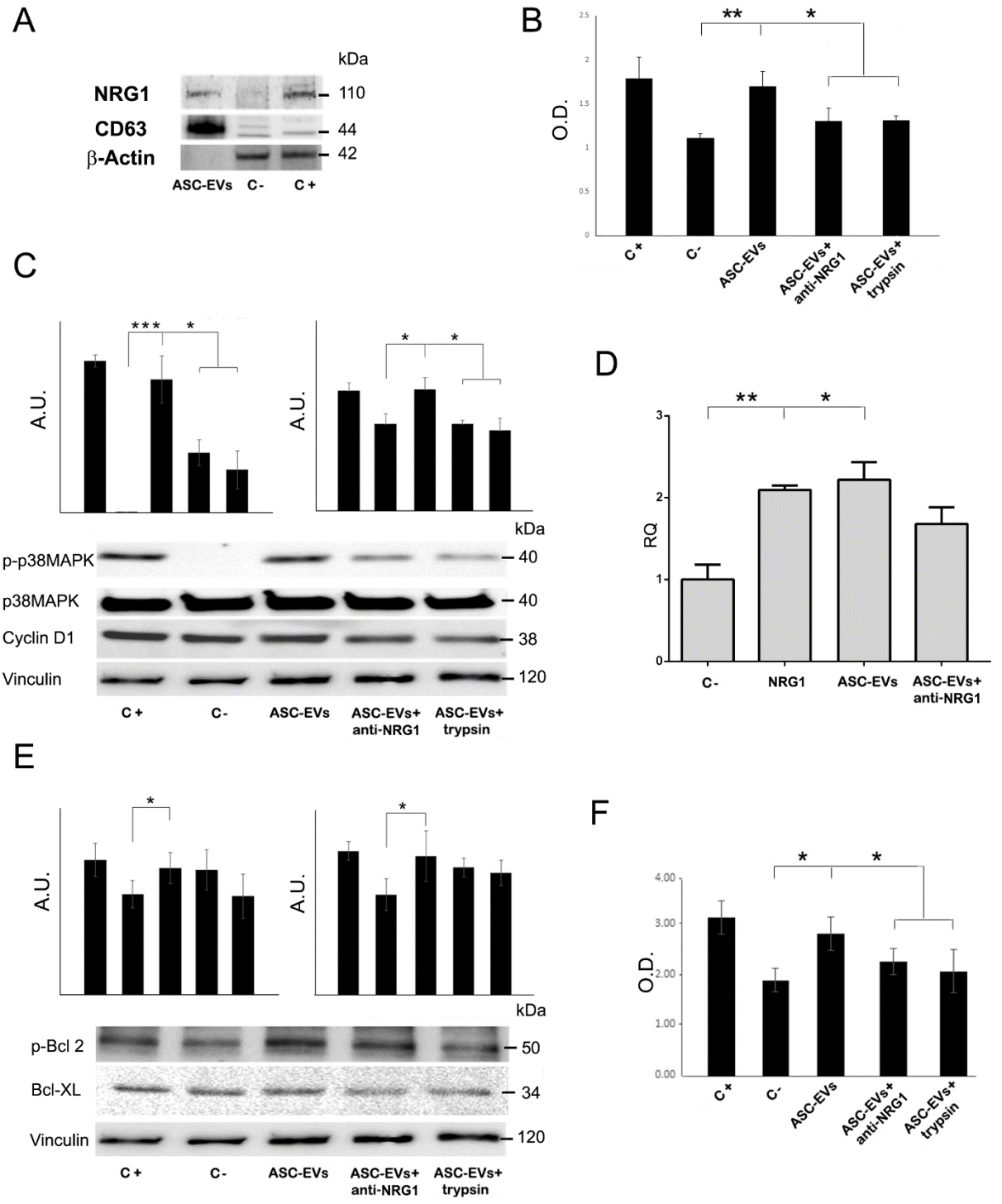
A
kDa
NRG1
110
CD63
44
β-Actin
42
ASC-EVs
C-
C+
B
O.D.
**
*
C+
C-
ASC-EVs
ASC-EVs+ anti-NRG1
ASC-EVs+ trypsin
C
A.U.
***
*
A.U.
*
*
kDa
p-p38MAPK
40
p38MAPK
40
Cyclin D1
38
Vinculin
120
C+
C-
ASC-EVs
ASC-EVs+ anti-NRG1
ASC-EVs+ trypsin
D
RQ
**
*
C-
NRG1
ASC-EVs
ASC-EVs+ anti-NRG1
E
A.U.
*
A.U.
*
kDa
p-Bcl 2
50
Bcl-XL
34
Vinculin
120
C+
C-
ASC-EVs
ASC-EVs+ anti-NRG1
ASC-EVs+ trypsin
F
O.D.
*
*
C+
C-
ASC-EVs
ASC-EVs+ anti-NRG1
ASC-EVs+ trypsin

Figure 4

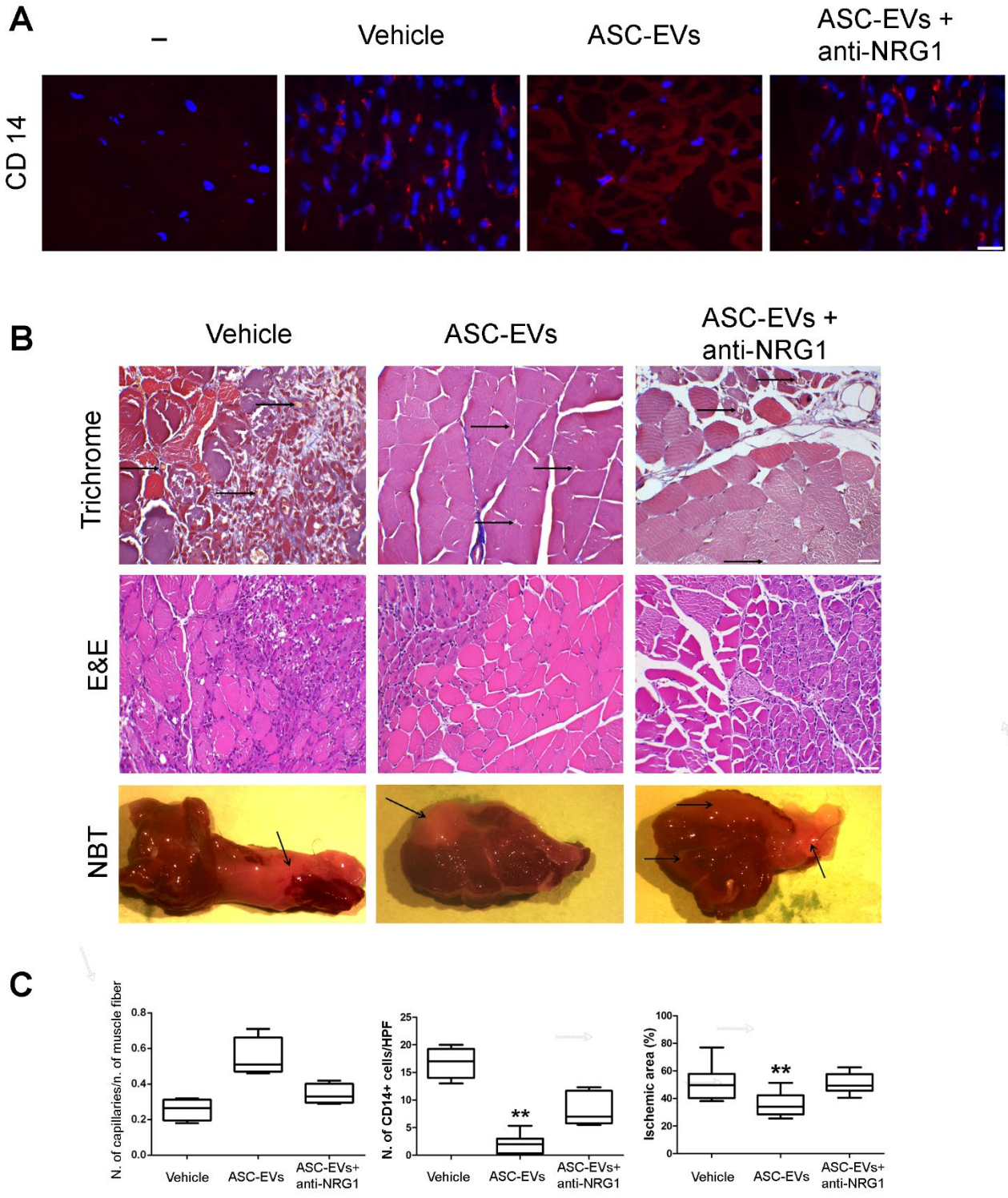
A
–
Vehicle
ASC-EVs
ASC-EVs + anti-NRG1
CD 14
B
Vehicle
ASC-EVs
ASC-EVs + anti-NRG1
Trichrome
E&E
NBT
C
N. of capillaries/n. of muscle fiber
0.8
0.6
0.4
0.2
0.0
Vehicle
ASC-EVs
ASC-EVs+ anti-NRG1
N. of CD14+ cells/HPF
25
20
15
10
5
0
**
Vehicle
ASC-EVs
ASC-EVs+ anti-NRG1
Ischemic area (%)
100
80
60
40
20
0
**
Vehicle
ASC-EVs
ASC-EVs+ anti-NRG1

Figure 5

A

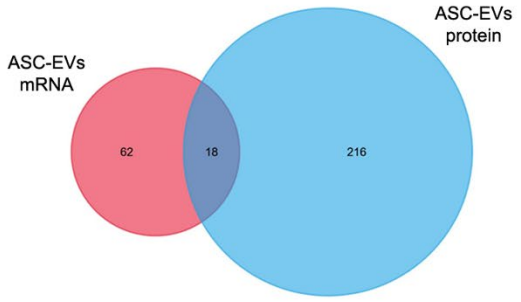

B

Gene symbol	Description
FN1	fibronectin 1
MMP2	matrix metallopeptidase 2
PLG	plasminogen
CXCL9	chemokine (C-X-C motif) ligand 9
ITGAV	integrin, alpha V
FLT1	fms-related tyrosine kinase 1
CXCL8	chemokine (C-X-C motif) ligand 8
IFNG	interferon, gamma
ANGPT1	angiopoietin 1
IL6	interleukin 6
THBS2	thrombospondin 2
TGFB1	transforming growth factor, beta 1
COL18A1	collagen, type XVIII, alpha 1
ADGRB1	adhesion G protein-coupled receptor B1
ENG	endoglin
CCL2	chemokine (C-C motif) ligand 2
TNF	tumor necrosis factor
S1PR1	sphingosine-1-phosphate receptor 1

C

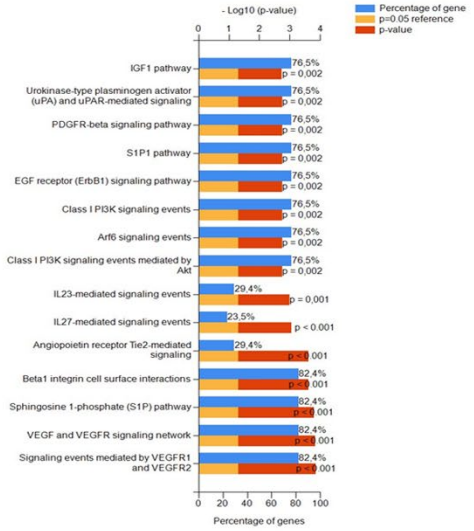

D

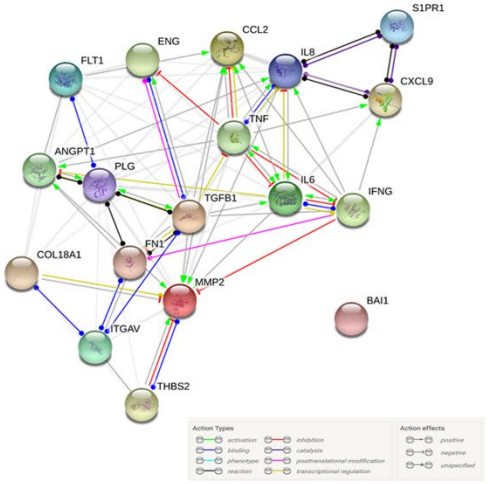

Figure 6

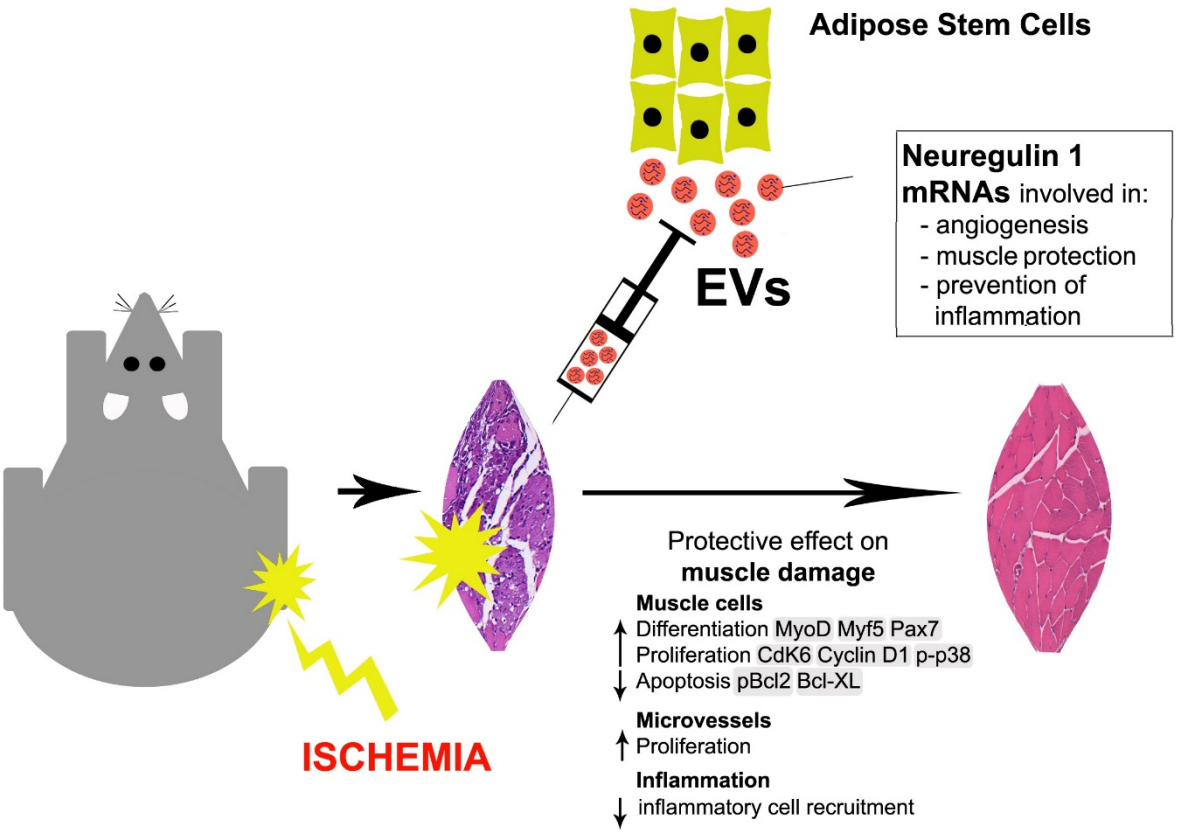
Adipose Stem Cells
Neuregulin 1
mRNAs involved in:
- angiogenesis
- muscle protection
- prevention of inflammation
EVs
ISCHEMIA
Protective effect on
muscle damage
Muscle cells
Differentiation MyoD Myf5 Pax7
Proliferation CdK6 Cyclin D1 p-p38
Apoptosis pBcl2 Bcl-XL
Microvessels
Proliferation
Inflammation
inflammatory cell recruitment

SUPPLEMENTAL MATERIALS

EXTRACELLULAR VESICLES FROM ADIPOSE STEM CELLS PREVENT MUSCLE DAMAGE AND INFLAMMATION IN A MOUSE MODEL OF HIND LIMB ISCHEMIA: ROLE OF NEUREGULIN-1

Federico Figliolini[1], Andrea Ranghino[2], Cristina Grange[2], Massimo Cedrino[1], Marta Tapparo[2], Claudia Cavallari[1], Andrea Rossi[2], Gabriele Togliatto[2], Saveria Femminò[2], Maria Vittoria Gugliuzza[2], Giovanni Camussi[2]* and Maria Felice Brizzi[2]*

[1]2i3T Scarl University of Turin, [2]Department of Medical Sciences, University of Turin, Turin, Italy

List of primer used in qRT-PCR

Gene name	Forward Primer (5'->3')	Reverse Primer (5'->3')
m-MyoD	TACAGTGGCGACTCAGATGC	GAGATGCGCTCCACTATGCT
m-Myogenin	CTACAGGCCTTGCTCAGCTC	ACGATGGACGTAAGGGAGTG
m-Myf5	GACGGCATGCCTGAATGTAAC	CAAGCAATCCAAGCTGGACAC
m-Pax7	CCTCCATGTCACCTCAAGTAGCT	ACAAACAGCACAACATCACATTTTC
m-p21	GCAGACCAGCCTGACAGATTT	ACAGCAGAAGAGGGCGGG
m-p27	GCGACCTGCTGCAGAAGATT	GCTTCTTGGGCGTCTGCTC
m-Egr1	GAGCACCTGACCACAGAGTCC	AGGCAACCGAGTCGTTTGG
h-EGR1	CCGCAGAGTCTTTTCCTGACA	CCACAAGGTGTTGCCACTGT
m-Nrg1	TCAGCAAGTTAGGAAACGACAG	ACATAAGGTCTTTCAGTTGAGGC
h-NRG1	ACTTGTGCAAGTGCCCAAATG	TGCAGATGCCGGTTATGGT
h-GAPDH	TGGAAGGACTCATGACCACAGT	CATCACGCCACAGTTTCCC
h-ACTB	TGAAGATCAAGATCATTGCTCCTC	CACATCTGCTGGAAGGTGGAC
m-GAPDH	TGTCAAGCTCATTTCCTGGTATGA	TCTTACTCCTTGGAGGCCATGT
m-ACTB	GATTACTGCTCTGGCTCCTAGCA	GCCACCGATCCACACAGAGT

Supplemental Materials and Methods

***In vivo* model of hind limb ischemia (HLI)**

Animal studies were conducted in accordance with the Italian National Institute of Health Guide for the Care and Use of Laboratory Animals. All procedures were approved by the Ethics Committee of the University of Turin and the Italian Health Ministry (authorization number: 490/2015-PR). Mice were housed according to the Federation of European Laboratory Animal Science Association Guidelines. All experiments were performed in accordance with relevant guidelines and regulations. C57BL/6J male mice (Charles River Laboratories), aged 7 to 8 weeks were used. Since the female estrus cycle could introduce unexpected variables, only male mice have been used in this study. Hind limb ischemia was performed as previously described[1]. Briefly, a small skin incision was performed on the middle portion of the left hind limb of each mouse under sterile conditions. The proximal end of the left femoral artery and the distal portion of the saphenous artery were ligated, dissected and excised. The overlying skin was then closed using a sterilized 6-0 silk suture[2]. Two different ASC-EV administration routes were used in the preliminary study: route 1: ASC-EVs ($2x10^{10}$/mouse) were injected as detailed: $1x10^{10}$ administrated intravenously immediately after intervention (T0), $0.5x10^{10}$ via intramuscular injection on day 1 (T1) and again on day 2 (T2); route 2: ASC-EVs were injected intramuscularly at 1 $x10^{10}$ immediately after surgery (T0), and at $0.5x10^{10}$ at day 1 (T1) and day 2 (T2) (n=8/each group/protocol). Animals were sacrificed on either day 3 (T3) or day 7 (T7) for molecular and histological analyses (n=8/group). In selected experiments, ASC-EVs pretreated with a blocking antibody against neuregulin 1 (NRG1) (Raybiotech) were used (n=8). Semi-quantitative estimations (by repeated measures, analyzed using the ANOVA and Newman-Keuls Multiple Comparison tests) of foot damage were performed serially using the following classification: 3=dragging of foot (foot necrosis); 2=no dragging, but no

plantar flexion (foot damage); 1=plantar flexion, but no toe flexion (toe damage); and 0=flexing the toes to resist gentle traction on the tail (no damage)[3]. To assess the area of muscle damage, at day 7 muscles were rapidly removed and incubated for 20 min at 37°C in 0.1% solution of nitro-blue tetrazolium in phosphate buffer. The necrotic mass was expressed as a percentage of total muscle mass (n=4 each/group protocol)[4].

Histological and immunofluorescence analyses

Gastrocnemius muscle sections from ischemic and normo-perfused limbs were stained with hematoxylin and eosin and Masson's trichrome for histological analysis. Images of all the injured areas of the ischemic limb sections were acquired for total muscle fiber counts. Random images from total, non-ischemic limb sections were used as controls. Data were quantified as percentage of damage area over total area. Capillary density was calculated as the number of capillaries per muscle fiber in Masson's trichrome sections. Ten randomly chosen microscopic fields, from three different sections in each tissue block, were examined and count by two blind observers using Image J software. Capillary density was expressed as the number of capillaries per muscle fiber ± SEM (Magnification: x400). Inflammatory cells in gastrocnemius muscles were quantified using immunofluorescence analyses. Muscle samples were embedded in OCT compound (Bio-Optica) and snap-frozen in liquid nitrogen. Tissue slices (5 µm in thickness) were stained a rat anti-mouse CD14 primary antibody (PharMingen). Anti-rat Alexa Fluor Texas red (Molecular Probe) was used as secondary antibody. Hoechst dye was added for nuclear staining. Fifteen randomly chosen microscopic fields, from three different sections in each tissue block, were examined for inflammatory cell count by two blind observers. Inflammation was expressed as the number of CD14 positive cells per high power field (HPF) ± SEM (Magnification: x400).

Muscle cell proliferation was evaluated by immunohistochemistry. Gastrocnemious muscle sections of paraffin-embedded samples were stained with a monoclonal anti-proliferating

Cell Nuclear Antigen (anti-PCNA) antibody (Santa Cruz) at day 7. Apoptosis was evaluated using the TUNEL assay (ApopTagOncor, Gaithersburg, MD), accordingly with the manufacture's protocol. Number of PCNA-positive cells and TUNEL-positive nuclei were evaluated by counting the number of positive nuclei per field in 10 randomly chosen sections using ImageJ software.

Isolation and characterization of ASC-EVs

Male-derived ASCs were purchased from Lonza and cultured in ADSC growth medium (Lonza) in T75 flasks. For EV isolation, ASCs (passage 2–7 and 60-70% of confluence) were washed several times with PBS (Lonza), to eliminate traces of serum and then cultured in alpha MEM (Lonza) with penicillin/streptomycin (both from Sigma) and L-glutamine (Sigma-Aldrich, St. Louis, MO) without FBS overnight (16 hours) in 5%CO_2 incubator at 37°C. Cell culture supernatants (8 ml each T75 flask) were centrifuged twice at 4000 g, for 10 min, at 4°C and submitted to microfiltration (0.22 μm PES from Meck Millipore, Tullagreen, Ireland) to eliminate cell debris and apoptotic bodies, and then ultracentrifuged at 100.000 g, for 2 hours, at 4°C in a Beckman Coulter Optima L-90K ultracentrifuge with rotor 70 Ti in polycarbonate tubes (355618) (Beckman Coulter, Indianapolis, IN). Pellets were resuspended in alpha MEM supplemented with 1% DMSO and stored at -80°C for further experiments. In selected experiments, ASC-EVs were either treated with anti-NRG1 blocking antibody (Raybiotech) 5ug/ml for 1 hour at RT, or with trypsin 0.1X (0.025% w/v) for 1 hour at 37°C, then washed with PBS, re-ultracentrifuged at 100.000 rcf for 2 hours, at 4°C and resuspended, as previously described.

In order to perform Nanosight Tracking Analyses (NTA), ASC-EVs were diluted (1:200) in sterile saline solution (0.9%) filtered with 0.1μm pore filter and analysed using a NanoSight NS300 equipped with NTA Analytical Software (Malvern Panalytical Ltd., Malvern, UK). Three videos of 30 s duration were recorded for each sample, and camera levels were set

for all the acquisition at 16. NTA post-acquisition settings were maintained constant among all samples, and videos were then analyzed to measure EV mean, mode, median (D50), and concentration.

The number of ASC-EVs released *per* cell was calculated as follow: the EV concentration (EVs/ml) acquired by the Nanosight analysis was multiplied by the EV preparation volume (ml). This corresponds to the total EV number/preparation. To obtain the EV number released *per* cell, the total EV number was divided by the ASC number overnight starved.

Guava FACS analysis

The characterization of EV surface molecules was performed by GUAVA FACS analysis (GUAVA EasyCyte 8, Millipore) using MACSPlex exosome kit (Miltenyi biotech). Briefly, ASC-EVs were incubated with the antibody-coated capture Beads and subsequently ASC-EVs, bound to the MACSPlex Exosome Capture Beads, were labeled with the MACSPlex Exosome Detection Reagents containing different antibodies recognizing different surface markers. Control antibodies were also used. Consequently, the sandwich complexes formed among the MACSPlex Exosome Capture Bead, ASC-EVs, and the detection reagent were analyzed based on the fluorescence generated by the MACSPlex Exosome Capture Bead and the detection reagents. ASC-EVs fluorescence mean intensity was analysed for each antibody and compared to the controls following manufacturer's instruction.

NRG1 ELISA assay

ELISA assay was performed on protein derived from different ASC-EV preparations. Briefly, 100µl of ASC-EV proteins were loaded in a microtiter plate provided by NRG-1 ELISA kit (mybiosource) that has been coated with an anti-NRG-1 specific antibody. After incubation, biotin-conjugated antibody and the avidin-coniugated HRP were added. The reaction was blocked by the addition of sulphuric acid solution and then measured spectrophotometrically

at a wavelength of 450nm. NRG1 concentration, in each sample, was determined by comparing the O.D. of the sample to the standard curve. In order to obtain the NRG1 content in ASC-EVs ($1x10^{10}$), the NRG1 concentration was multiplied by the volume and by the dilution of the analyzed sample and normalized for the number of EVs from which protein sample derived.

Molecular characterization of ASC-EV cargo

ASC-EV proteins from different preparations (n=8) were extracted using a lysis buffer provided by the Human L1000 (Glass Slide) protein array kit (Ray biotech). Protein quantification was carried out using the BCA protein assay (Thermo Fisher), which was performed according to the manufacturer's protocol. This kit allows the detection of 1,000 different proteins, including cytokines, chemokines, adipokines, growth factors, angiogenic factors, proteases, soluble receptors, adhesion molecules and other proteins to be simultaneously investigated. Approximately 25 µg of protein were loaded for each sample. The fluorescence signal was subjected to background subtraction and the cut-off threshold was set as > 150 Fluorescence Intensity AU.

A PCR angiogenesis array was performed on total RNA that had been extracted from ASC-EVs (n=7) using a miRVANA isolation kit and quantified using a NanoDrop1000 spectrophotometer. The RT^2 First Strand kit (SABiosciences) was employed for cDNA synthesis, according to manufacturer's instructions. Two hundred ng of cDNA was run on an Angiogenesis RT^2 Profiler PCR Array (PAHS 024, PAMM-099Z, Qiagen, Frederick, MD, USA) to profile 84 key genes involved in angiogenesis (list of genes available on website: http://www.sabiosciences.com).

Data from the protein and mRNA arrays were compared and pathway enrichment analysis was performed using Funrich 3.1.3[18]. Data were considered significant at $p<0.05$

(Hypergeometric test with Bonferroni correction). Interaction network on selected proteins/genes was built using STRING online software.

***In vitro* assays**

In vitro hypoxia model. The following *in vitro* model was used to simulate ischemia/reoxygenation (I/R) injury *in vitro*: cells (C2C12, differentiated myoblasts or HMECs) were cultured in a hypoxic gas mixture (1% O_2) for 8 hours in normal culture medium both with and without FBS. After hypoxia, cells were cultured in normoxic conditions, both with and without ASC-EVs (10,000 EVs/target cell), for 16 hours and then analyzed for proliferation, apoptosis, RNA and protein expression for 6 days, for the differentiation experiments as described below.

Myoblast differentiation into myotubes: C2C12 were cultured in DMEM high glucose (4.5 g/L-Lonza, Basel, Switzerland) and 20% FBS (Lonza). When cells reached 80% confluence, cells were cultured in high glucose + 2% horse serum DMEM for 6 days. In selected experiments, C2C12 were cultured in hypoxic gas mixture (1% O_2) for 8 hours and then cultured in normoxic conditions, both with and without 2% horse serum and ASC-EVs, for 6 days.

Proliferation: C2C12 and HMEC proliferation was performed via 5-bromo-2-deoxyuridine (BrdU) (Roche Diagnostics, Mannheim, Germany) incorporation in cells cultured in hypoxic conditions and incubated both with and without ASC-EVs. Briefly, cells were plated in 96 well plates, cultured in hypoxic gas mixture (1% O_2) for 8 hours, cultured in normoxic conditions, both with and without ASC-EVs, for 16 hours and then analyzed for BrdU incorporation.

Apoptosis analysis in myoblasts and myotubes: C2C12 apoptosis was analysed using MUSE CELL Analyzer (Millipore), and a double staining with Annexin V and 7AAD. Briefly,

cells were plated in 6 well plates, cultured in hypoxic gas mixture (1% O_2) for 8 hours and then cultured in normoxic conditions, both with and without ASC-EVs, for 16 hours and then analyzed. Myotube apoptosis was evaluated by counting the fragmented nuclei stained with Hoechst staining. Briefly, differentiated C2C12, plated in 6 well plates, were cultured in hypoxic gas mixture (1% O_2) for 8 hours and then cultured in normoxic conditions, both with and without ASC-EVs, for 16 hours. Cells were then fixed and stained with Hoechst staining. Normal and fragmented nuclei were counted in microphotographs that were obtained using a fluorescence microscope, and the percentage of apoptotic cells was calculate as the ratio between the number of fragmented nuclei and the number of total nuclei per microscopic field. In selected experiments ASC-EVs pretreated with a blocking NRG1 antibody, trypsin (0.25% w/v) and rhNRG1 (45 pg equivalent to $1.5x10^9$ ASC-EVs/$1.5x10^5$ cells) were used.

RT-PCR array analysis

The Skeletal Muscle Myogenesis and Myopathy RT^2 Profiler PCR Array (PAMM-099Z, Qiagen) was used to characterize the gene expression profiles of the healthy and ischemic gastrocnemius muscles of C57BL/6J, both those treated with ASC-EVs and those untreated. Briefly, according to manufacturer's instructions, RNA extracted from mouse muscles using the miRVANA kit was treated with gDNA elimination buffer to degrade DNA contamination, and then reverse-transcripted using RT^2 First Strand kit. RT products were loaded into 96 well arrays, and Real Time RT-PCR amplification was performed using the StepOne Plus (Applied Biosystem) Real Time PCR System. Data analysis was performed using the RT^2Profiler PCR Array Data Analysis tool provided by the manufacturer (SABioscience). The expression levels of each gene were normalized for housekeeping genes, according to manufacturer's instructions.

Real Time PCR analysis

The total RNA from the ischemic gastrocnemius muscles of C57BL/6J and hypoxic C2C12 (both those treated with ASC-EVs and those untreated, as previously described) was extracted using miRVANA RNA extraction kit and then reverse-transcripted using High-Capacity cDNA Reverse Transcription Kit (Applied Biosystem). The cDNA of the various samples was loaded into 96 well plates with different primers for mouse MyoD, Myogenin, Myf5, Pax7, p21 and p27 (*online Data Supplement* Table I), and Real Time RT-PCR amplification was performed using the StepOne Plus (Applied Biosystem) Real Time PCR System. Data analysis was performed using ExpressionSuite software (Life Technologies) and the expression levels of each gene were normalized for housekeeping genes. In selected experiments the expression of the early growth response 1 (EGR1) gene was evaluated as indicated. The primer sequences are reported in the *online Data Supplement*, Table I.

Western Blot

ASC-EVs, C2C12 and SCs, stimulated as indicated, were lysed in lysis buffer (RIPA buffer with proteinase inhibitors, Sigma Aldrich) for 1 hour at 4°C and centrifuged at 10,000 rcf. The supernatants were collected, quantified using the Bradford method and analyzed by western blot. Western blot analyses were performed using (4-15%) SDS-PAGE electrophoresis gel (Biorad) and blotted with an iBLOT device (Invitrogen) onto nitrocellulose membrane filters. The following primary antibodies were used: NRG1 (Raybiotech), CD63, MyoD, myogenin, CdK6, pho-p38MAPK, p38MAPK, Cyclin D1, p-Bcl-2, Bcl-XL, □-actin and vinculin (Santa Cruz). Densitrometric analysis was performed by Image Lab™ Software (BioRad) and data were expressed as arbitrary unit ± SD.

Supplemental Figure 1

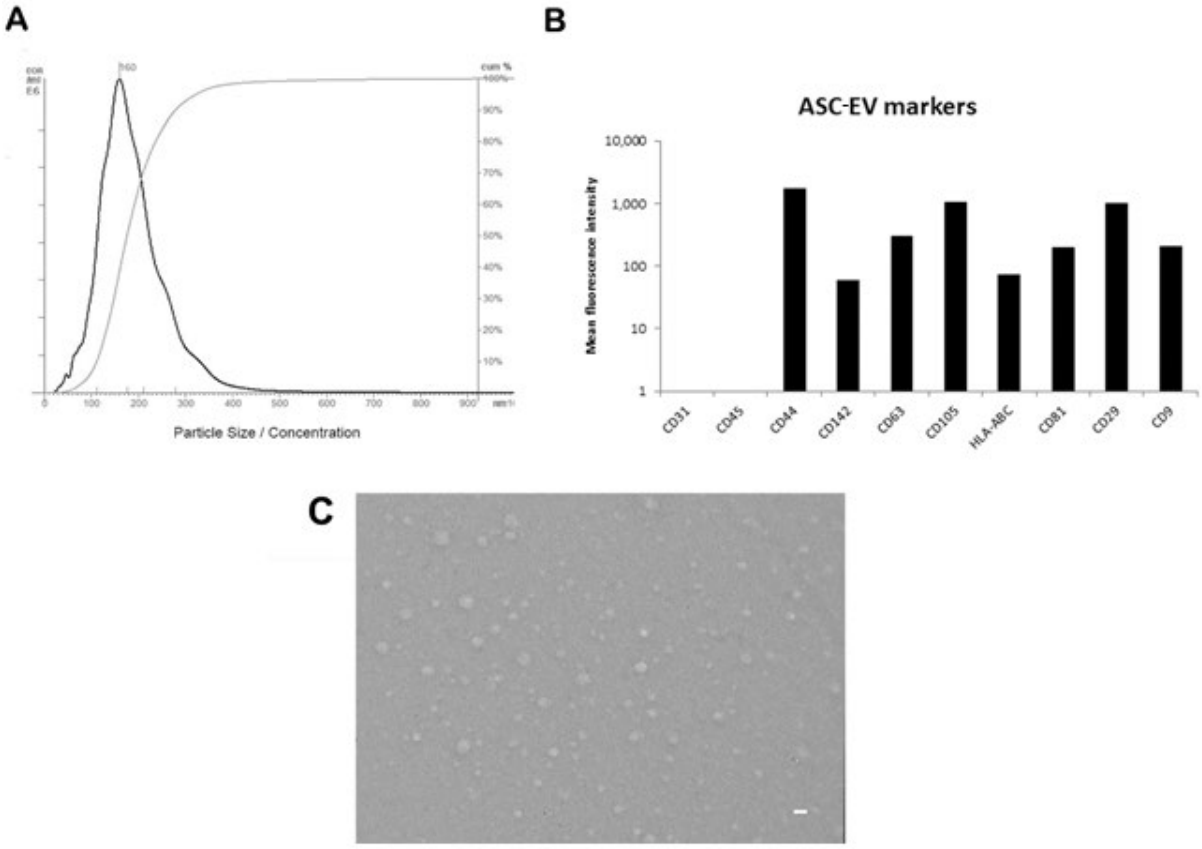

Supplemental Figure 1. Characterization of ASC-EVs. A, Representative image of Nanosight analysis of ASC-EVs. **B,** GUAVA FACS analysis of ASC-EVs for expression different exosomal and non exosomal markers by MACSPlex exosome kit. **C,** Representative transmission electron microscopy imaging of ASC-EV. JEOL Jem 1010 electron microscope (Magnification 75k) was used (white bars= 100 nm).

Supplemental Figure 2

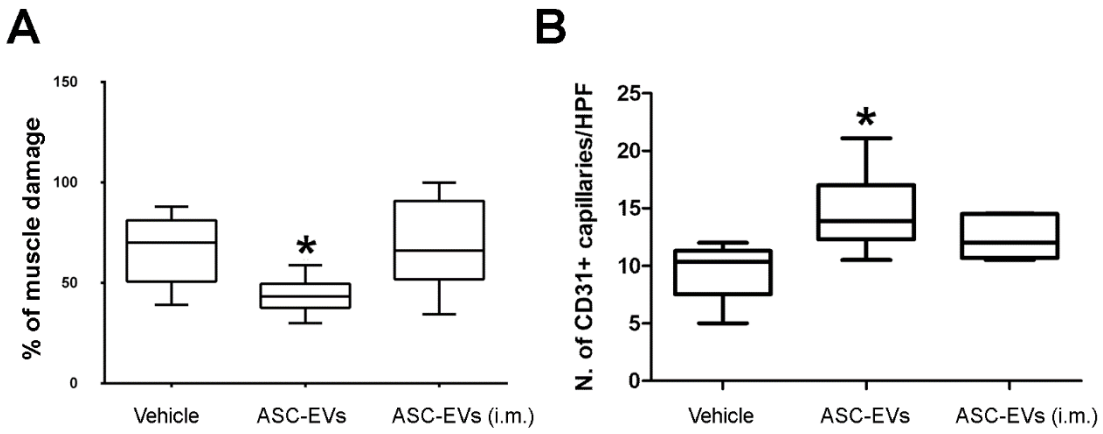

Supplemental Figure 2. Comparison between different routes of ASC-EV administration. **A,** Two different administration routes were compared. Route 1 (ASC-EVs): $1x10^{10}$ administrated intravenously immediately after intervention (T0), $0.5x10^{10}$ via intramuscular administration on day 1 (T1), and again on day 2 (T2); route 2: EVs were administered intramuscularly with the same timing and doses (T0:$1x10^{10}$; T1:$0.5x10^{10}$; T2:$0.5x10^{10}$) (ASC-EVs i.m). Quantitative analysis of muscle damage areas in hematoxilin-eosin stained gastrocnemius muscles of ischemic hind limbs at day 7 after surgery in Vehicle, ASC-EV and ASC-EV (i.m.) treated animals. Data are expressed as percentage of damage area ± SEM; *p value < 0.05 ASC-EVs (i.v) vs Vehicle, (One way Anova - Newman-Keuls Multiple Comparison Test) (n=8/each treatment) (left panel). **B,** Quantitative analyses of CD31+ capillaries in Vehicle, ASC-EV (i.v.) and ASC-EV (i.m.) ischemic hind limb at day 7 after surgery. Data are expressed as mean ± SEM; *p value < 0.05, ASC-EVs (i.v) vs Vehicle, (One-Way Anova - Newman-Keuls Multiple Comparison Test) (n=8/each treatment) (right panel).

Supplemental Figure 3

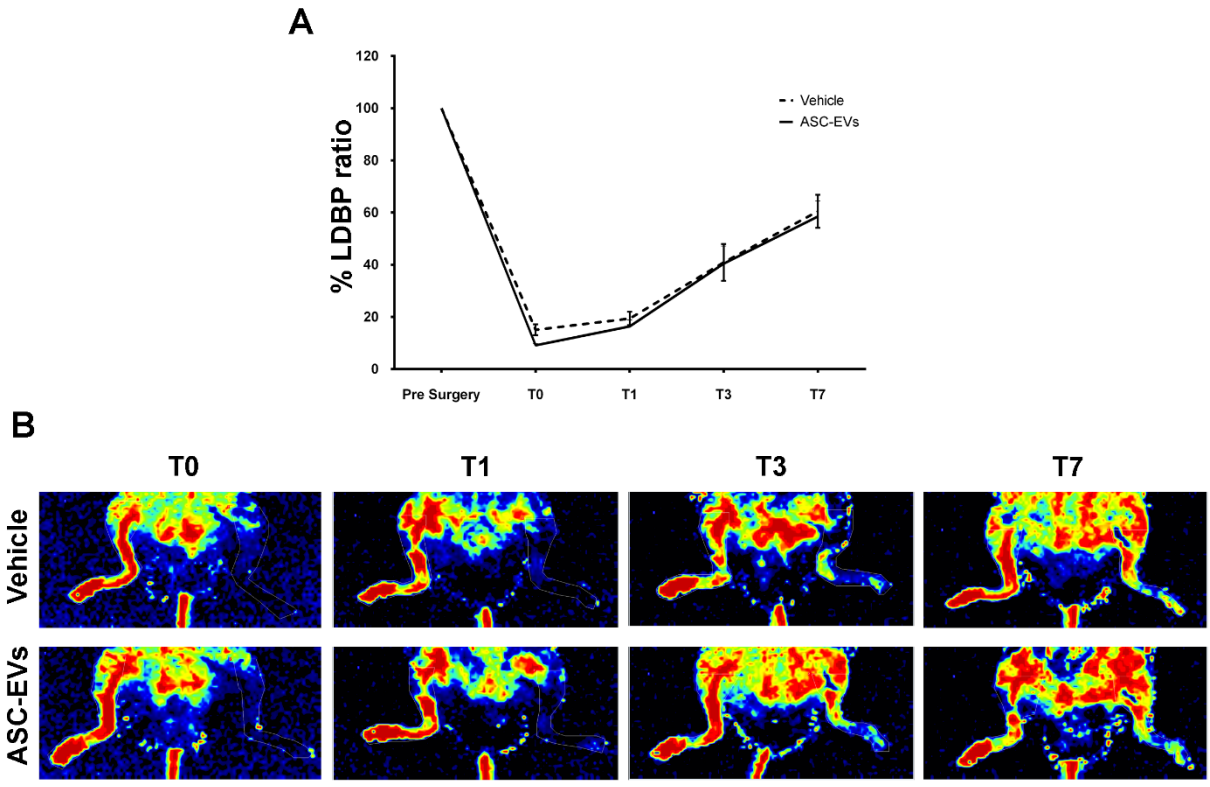

Supplemental Figure 3. Laser Doppler Blood Perfusion analysis. A, Quantitative analysis of blood perfusion measured by LDBP at different time points (T0, T1, T3 and T7). Data are expressed as mean ± SD. **B,** Representative images of Laser Doppler Blood Perfusion (LDBP) obtained immediately after intervention (T0), and at day 1 (T1), day 3 (T3), and day 7 (T7) of mice treated with Vehicle and ASC-EVs.

Supplemental Figure 4

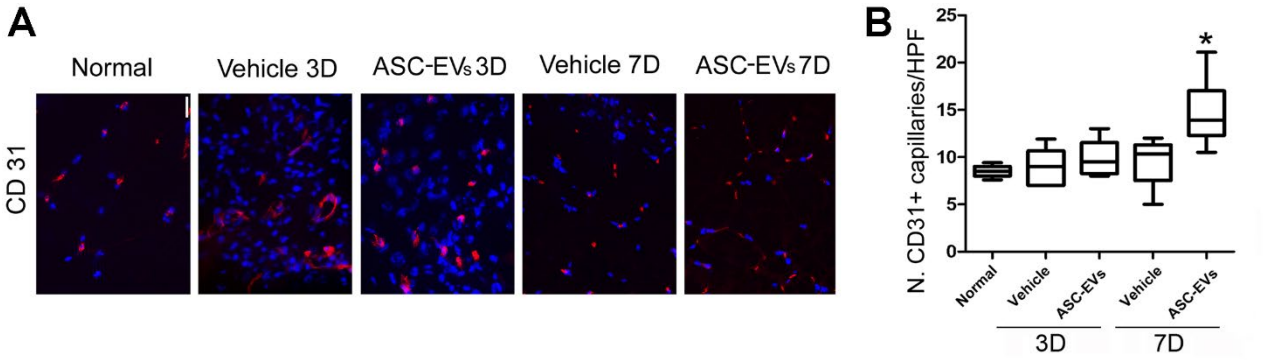

Supplemental Figure 4. **Analysis of capillary density. A,** Representative images and **B,** quantitative analyses of CD31+ capillaries in Vehicle and ASC-EV treated mice at day 3 and 7 after surgery. Data are expressed as mean ± SEM; *p value < 0.05, ASC-EVs vs Vehicle, (One-Way Anova - Newman-Keuls Multiple Comparison Test) (n=8/each group) (right panel).

Supplemental Figure 5

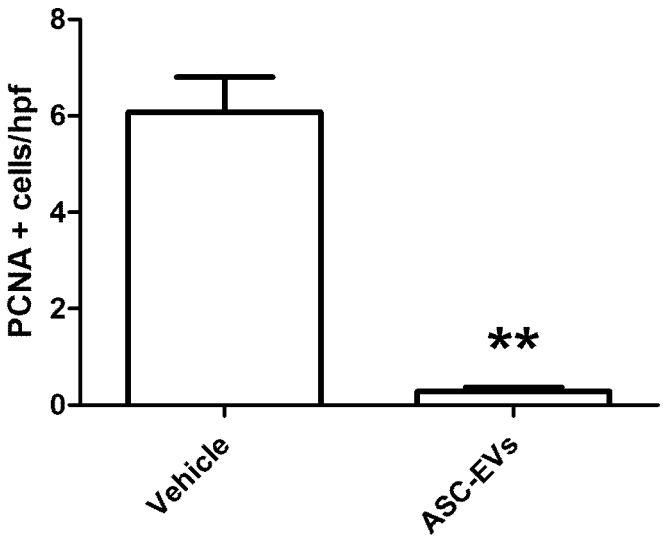

Supplemental Figure 5. *In vivo* PCNA quantification. Quantification of PCNA positive nuclei/hpf, analyzed in 10 randomly images of ischemic hind limbs at day 7 after surgery in Vehicle and ASC-EVs treated animals. Data are expressed as the mean of positive PCNA nuclei ± SEM; **p value < 0.001 ASC-EVs vs Vehicle (Test T student) (n=6).

Supplemental Figure 6

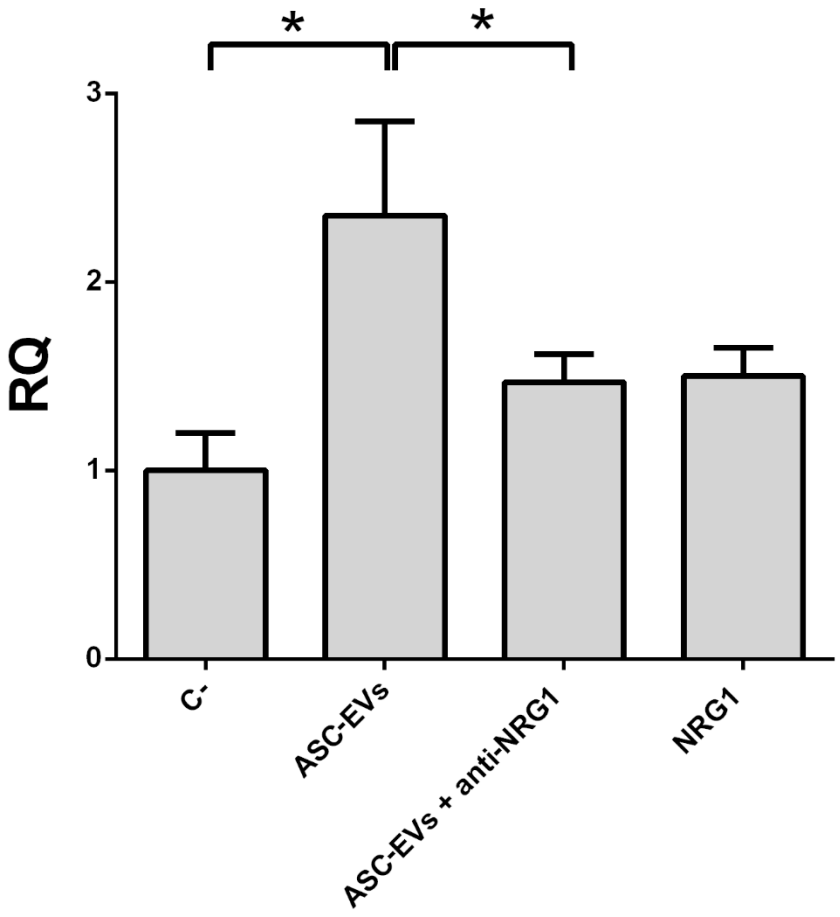

Supplemental Figure 6. EGR1 gene expression. qRT-PCR analysis of endothelial cells cultured in hypoxic condition, without FBS (C-), with rhNRG1 (NRG1), in presence of ASC-EVs (ASC-EVs) and ASC-EVs pretreated with an anti-NRG1 blocking antibody (ASC-EVs + anti-NRG1) (n=3 *$p<0.05$ C- and ASC-EVs+anti-NRG1 vs ASC-EVs).

Supplemental Figure 7

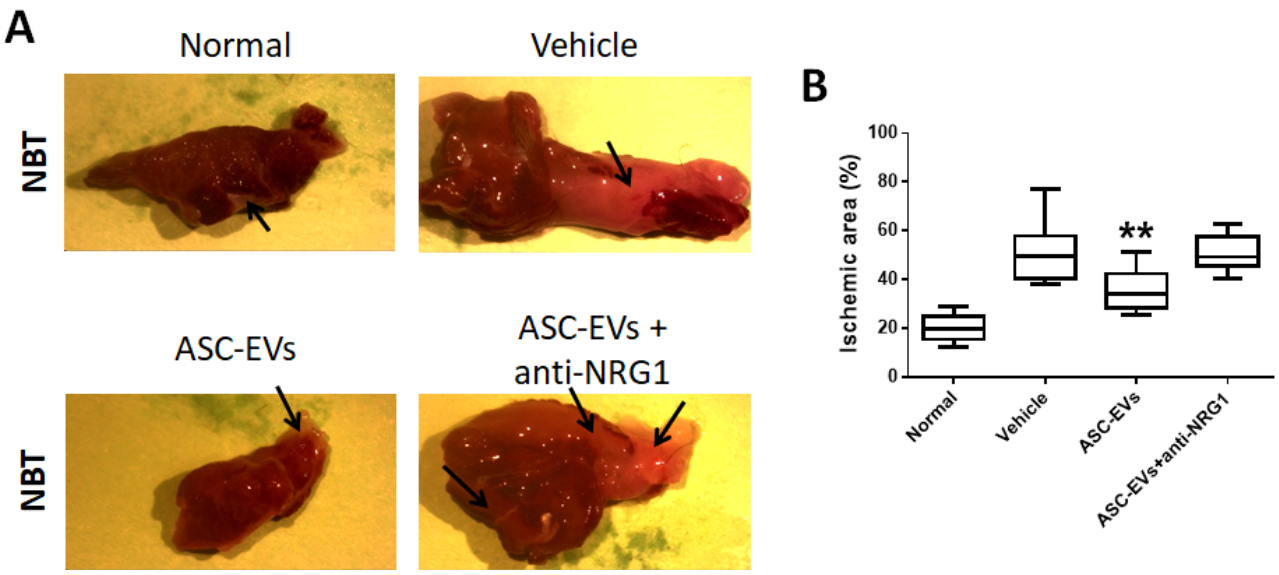

Supplemental Figure 7. Analysis of ischemic area in muscles. A, Representative NTB images of gastrocnemius muscles from normal or ischemic hind limb in vehicle, ASC-EVs and ASC-EVs + anti-NRG1 treated animal, as indicated. Arrows indicate the ischemic area in the NTB sections. **B,** Quantitative analysis of the percentage of the ischemic area in normal and ischemic hind limb in Vehicle, ASC-EV and ASC-EV + anti-NRG1 treated animals at day 7. Data are expressed as mean ± SEM; *p value < 0.05 **p<0.01, ASC-EVs vs Vehicle, (One-Way Anova - Newman-Keuls Multiple Comparison Test) (n=4 for NTB analysis).

Supplemental Figure 8

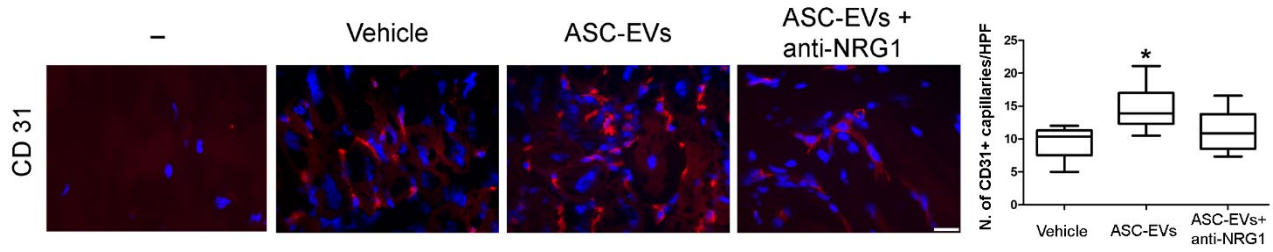

Supplemental Figure 8. Analysis of capillary density. Representative immunofluorescence images of neoangiogenesis. Anti-CD31mAb was used to analyze gastrocnemius muscles of ischemic hind-limb in Vehicle, ASC-EVs- and ASC-EVs + anti-NRG1 treated animals as indicated (Original Magnification: X400 - scale bar: 25 μm). The negative control for primary antibody is indicated as"-".

Supplemental Table 1

ASC-EV treated vs. untreated muscles								
Gene Symbol	**Fold Regulation**	**SD**	**Gene Symbol**	**Fold Regulation**	**SD**	**Gene Symbol**	**Fold Regulation**	**SD**
Myod1	3.85	± 0.30	**Cryab**	1.28	± 0.17	**Dmd**	1.00	± 0.26
Myf5	2.97	± 0.18	**Myf6**	1.28	± 0.14	**Neb**	1.00	± 0.29
Il6	2.89	± 0.17	**Mb**	1.27	± 0.85	**Tnnt3**	0.99	± 0.3
Cav1	2.33	± 0.50	**Mmp9**	1.25	± 0.46	**Pax3**	0.97	± 0.13
Igf2	2.03	± 0.79	**Myot**	1.24	± 0.71	**Acvr2b**	0.96	± 0.27
Ppargc1a	1.71	± 0.59	**Tnnt1**	1.24	± 0.32	**Slc2a4**	0.96	± 0.36
Ppargc1b	1.71	± 0.78	**Akt1**	1.23	± 0.33	**Tnni2**	0.95	± 0.28
Igf1	1.69	± 0.49	**Dmpk**	1.23	± 0.54	**Ttn**	0.95	± 0.22
Ctnnb1	1.69	± 0.67	**Myog**	1.23	± 0.61	**Acta1**	0.88	± 0.41
Capn2	1.62	± 0.31	**Akt2**	1.20	± 0.4	**Adrb2**	0.87	± 0.49
Capn3	1.62	± 0.51	**Hk2**	1.18	± 0.67	**Igfbp5**	0.86	± 0.17
Prkaa1	1.61	± 0.58	**Ppp3ca**	1.18	± 0.33	**Myh2**	0.84	± 0.26
Lmna	1.58	± 0.24	**Tnnc1**	1.18	± 0.49	**Fbxo32**	0.82	± 0.41
Cs	1.57	± 0.81	**Rps6kb1**	1.16	± 0.31	**Actn3**	0.81	± 0.67
Il1b	1.55	± 0.30	**Pdk4**	1.15	± 0.42	**Igfbp3**	0.81	± 0.24
Agrn	1.55	± 0.61	**Cav3**	1.14	± 0.56	**Sgca**	0.81	± 0.19
Mapk14	1.53	± 0.75	**Dag1**	1.14	± 0.12	**Nfkb1**	0.78	± 0.17
Prkag1	1.52	± 0.80	**Camk2g**	1.12	± 0.21	**Atp2a1**	0.74	± 0.1
Pax7	1.52	± 0.62	**Trim63**	1.12	± 0.27	**Prkag3**	0.74	± 0.28
Bmp4	1.49	± 0.35	**Hdac5**	1.11	± 0.41	**Nos2**	0.71	± 0.24
Mapk1	1.44	± 0.41	**Utrn**	1.11	± 0.31	**Adipoq**	0.70	± 0.3
Fgf2	1.38	± 0.29	**Foxo3**	1.10	± 0.59	**Tnf**	0.67	± 0.25
Mapk3	1.36	± 0.41	**Pparg**	1.10	± 0.74	**Ikbkb**	0.65	± 0.21
Des	1.35	± 0.26	**Dysf**	1.08	± 0.16	**Foxo1**	0.59	± 0.15
Musk	1.34	± 0.19	**Mef2c**	1.06	± 0.32	**Myh1**	0.56	± 0.18
Mapk8	1.33	± 0.49	**Prkab2**	1.06	± 0.43	**Tgfb1**	0.54	± 0.25
Cast	1.30	± 0.37	**Casp3**	1.05	± 0.36	**Lep**	0.24	± 0.19
Rhoa	1.29	± 0.49	**Mstn**	1.03	± 0.31			

Supplemental Table 1. Complete list of mRNAs of ASC-EV-treated muscles, compared with untreated muscles. RQ (fold regulation) values are evaluated by $2^{-\Delta\Delta Ct}$ ± SD (n=4).

Supplemental Table 2

Protein	Gene Name	Fluorescence Intensity (arbitrary unit)	± SD
Neuregulin 1	**NRG1**	50176	10353.11
LAG-3	**LAG3**	1979	184.91
Amylin	**IAPP**	753	144.60
IL-21	**IL21**	647	88.75
IL-13	**IL13**	632	80.76
GDF11	**GDF11**	626	129.04
HGFR	**MET**	625	123.97
MSHa	**MSX1**	590	43.49
GDF3	**GDF3**	587	78.70
Granzyme A	**GZMA**	573	13.92
BD-1	**DEFB1**	563	54.33
GDF5	**GDF5**	556	73.55
GDF9	**GDF9**	552	80.80
MIP-3 beta	**CCL19**	539	153.82
GRO	**CXCL2**	533	21.26
IFN-gamma	**IFNG**	530	34.57
GDF8	**MSTN**	527	51.67
IL-5	**IL5**	512	27

BAFF R / TNFRSF13C	**TNFRSF13C**	502	671.60
BAI-1	**ADGRB1**	494	211.42
IL-7	**IL7**	491	491
CK-MB	**CKB**	482	387.85
Angiopoietin-1	**ANGPT1**	468	256.80
IL-2	**IL2**	462	229.14
GM-CSF	**CSF2**	459	406.63
IL-8	**CXCL8**	451	64
IL-1 alpha	**IL1A**	448	38.77
CD71	**TFRC**	445	55.86
IL-6	**IL6**	439	18.00
GDF1	**GDF1**	422	62.07
TGF-beta 1	**TGFB1**	410	125.05
MMP-20	**MMP20**	400	15.48
Clusterin	**CLU**	389	27.22
Mammaglobin A	**SCGB2A2**	389	123.39
CNTF	**CNTF**	388	32.50
IL-9	**IL9**	383	97.00
Erythropoietin	**EPX**	381	30.61
TNF-alpha	**TNF**	378	83.87
Factor XIII A	**F13A1**	377	164.40
CD30 / TNFRSF8	**TNFRSF8**	374	33.62
BMP-7	**BMP7**	373	49.89

Insulin R	**INSR**	363	20.00
C2	**C2**	359	52.33
IL-15	**IL15**	353	34.10
TNF-beta	**LTA**	350	152.63
GFR alpha-3	**GFRA3**	346	22.23
MIP-1b	**CCL4**	344	120.55
EDG-1	**S1PR1**	341	8.30
CNTF R alpha	**CNTFR**	339	38.03
Growth Hormone (GH)	**GH1**	335	3.11
CCL28 / VIC	**CCL28**	330	27.13
Alpha Lactalbumin	**LALBA**	327	20.15
VDUP-1	**TXNIP**	322	130.11
ENPP2	**ENPP2**	320	19.80
GREMLIN	**GREM1**	317	38.50
IL-2 R beta /CD122	**IL2RB**	306	115.03
Ubiquitin+1	**UBB**	306	33.64
CA 19-9	**MUC16**	304	6.01
LH	**LHCGR**	303	49.14
HCR / CRAM-A/B	**CCHCR1**	303	70.10
ALPP	**ALPP**	300	26.87
SERPING1	**SERPING1**	299	90.51
FGF-16	**FGF16**	295	7.38
GM-CSF R alpha	**CSF2RA**	295	63.37

PDGF R beta	**PDGFRB**	292	81.62
Glut5	**SLC2A5**	292	23.02
ACK1	**TNK2**	291	18.74
FGF-18	**FGF18**	291	71.40
Cytokeratin 19	**KRT19**	290	44.55
IL-1 sRI	**IL1R1**	286	23.75
BMP-5	**BMP5**	283	25.80
Aldolase C	**ALDOC**	282	7.42
FGF-10 / KGF-2	**FGF10**	282	57.91
Dkk-4	**DKK4**	282	64.94
IL-1 R6 / IL-1 Rrp2	**IL1RL2**	281	29.20
Troponin C	**TNNC1**	281	59.75
IL-1 R4 / ST2	**IL1RL1**	277	20.27
MIP 2	**CXCL2**	277	103.20
CHI3L1	**CHI3L1**	276	53.39
IL-17	**IL17A**	270	89.93
CPN2	**CPN2**	269	7.78
AgRP	**AGRP**	269	26.65
TRA-1-81	**PODXL**	267	98.99
PARC / CCL18	**CCL18**	266	74.35
A1BG	**A1BG**	265	1.06
TXK	**TXK**	263	83.44
CTLA-4 /CD152	**CTLA4**	263	26.25
IL-2 R gamma	**IL2RG**	262	76.99
MCP-1	**CCL2**	261	28.59

Ceruloplasmin	**CP**	261	42.07
VGF	**VGF**	260	98.29
Lyn	**LYN**	257	12.73
Btk	**BTK**	256	15.56
MMP-1	**MMP1**	255	281.03
ApoA4	**APOA4**	255	12.73
NPTX1	**NPTX1**	254	69.65
Endoglin / CD105	**ENG**	252	4.79
C-peptide	**INS**	251	12.02
FGF-17	**FGF17**	248	89.80
IL-10 R alpha	**IL10RA**	248	65.50
MINA	**RIOX2**	247	32.88
S100 A8/A9	**S100A8**	247	93.55
Tec	**TEC**	246	51.62
Chordin-Like 2	**CHRDL2**	245	16.98
Aldolase A	**ALDOA**	245	6.36
Calcitonin	**CALCA**	245	46.32
Creatinine	**CSH1**	244	14.50
CTACK / CCL27	**CCL27**	244	129.86
EphA4	**EPHA4**	243	97.23
P-selectin	**SELP**	240	46.44
MMP-8	**MMP8**	240	64.13
Follistatin	**FST**	238	5.44
Angiopoietin-like 1	**ANGPTL1**	238	2.49
MIG	**CXCL9**	238	49.49

TRAIL R1 / DR4 / TNFRSF10A	**TNFRSF10A**	238	77.52
TRAIL R2 / DR5 / TNFRSF10B	**TNFRSF10B**	237	58.00
BTC	**BTC**	235	29.94
NR3C3	**PRG**	235	94.75
Corticosteroid-binding globulin	**SERPINA6**	233	29.34
E-Selectin	**SELE**	232	73.82
ZAP70	**ZAP70**	231.75	118.44039
SAA	**SAA1**	230	92.69
Thrombospondin-2	**THBS2**	229	55.93
CBP	**CREBBP**	228	16.97
MMP-19	**MMP19**	228	177.26
CV-2 / Crossveinless-2	**BMPER**	227	40.20
ALCAM	**ALCAM**	227	181.37
GCSF	**CSF3**	225	13.87
TRA-1-60	**PODXL**	225	105.71
L-Selectin (CD62L)	**SELL**	224	86.46
BNP	**nppb**	224	15.91
Cryptic	**CFC1**	222	9.61
Angiostatin	**PLG**	221	17.68
TGF-beta 5	**TGFB5**	221	100.61
IL-11	**IL11**	221	66.35

Ntn1	**NTN1**	218	39.95
IL-20 R alpha	**IL20RA**	215	9.23
VEGF R1	**FLT1**	215	270.11
Glut1	**SLC2A1**	214	1.20
Kallikrein 2	**KLK2**	213	63.99
LPS	**IRF6**	212	53.74
FER	**FER**	211	29.34
IL-13 R alpha 1	**IL13RA1**	211	3.19
PDGF R alpha	**PDGFRA**	208	71.53
MATK	**MATK**	208	55.15
GLP-1	**ZGLP1**	208	37.48
Frizzled-1	**FZD1**	207	0.64
FRK	**FRK**	207	34.29
SHBG	**SHBG**	205	58.69
Glut2	**SLC2A2**	204	24.62
CD 163	**CD163**	204	57.54
LTF	**LTF**	202	27.22
MSP alpha Chain	**MST1**	202	29.56
Lck	**LCK**	200	94.54
BMP-8	**BMP8B**	199	2.11
Galectin-3	**LGALS3**	198	15.04
MAC-1	**ITGAM**	198	81.02
Hepassocin	**FGL1**	197	36.07
CCR3	**CCR3**	196	72.64
FGF-11	**FGF11**	196	19.47

ACTH	**POMC**	195	61.87
PEPSINOGEN I	**PGC**	195	35.36
ADAMTS-17	**ADAMTS17**	195	16.62
TPX	**TPO**	194	29.69
BNIP2	**BNIP2**	194	18.38
PPARg2	**PPARG**	193	62.23
FGF-13 1B	**FGF13**	193	49.61
ASPH	**ASPH**	193	10.96
Galanin	**GAL**	190	31.47
TACI / TNFRSF13B	**TNFRSF13B**	189	12.62
Musk	**MUSK**	186	31.21
IL-1 F10 / IL-1HY2	**IL1F10**	185	46.74
NRG2	**NRG2**	185	36.82
GASP-2 / WFIKKN	**WFIKKN1**	185	4.78
CLC	**CLC**	185	19.17
SLPI	**SLPI**	184	71.50
IL-1 R8	**IL1RAPL1**	184	3.37
Fibrinopeptide A	**FGA**	183	53.03
Fyn	**FYN**	182	25.46
Sonic Hedgehog (Shh N-terminal)	**SHH**	182	35.18
Itk	**ITK**	182	32.53
BMP-4	**BMP4**	181	57.69
Calbindin	**CALB1**	181	19.45
SDF-1 / CXCL12	**CXCL12**	181	76.15

IL-17RC	**IL17RC**	180	81.54
XEDAR	**EDA2R**	179	109.02
IL-23p19	**IL23A**	179	28.28
CCL14 / HCC-1 / HCC-3	**CCL14**	176	21.50
ADAMTS-4	**ADAMTS4**	175	2.47
CA 125	**MUC16**	173	27.93
Fibronectin	**FN1**	173	57.63
EMAP-II	**EML2**	173	5.22
ABL1	**abl1**	173	26.52
HSP27	**HSPB1**	173	54.09
PI 3Kinase p85 beta	**PIK3R1**	172	43.84
Frizzled-3	**FZD3**	172	23.61
IL-1 sRII	**IL1R2**	171	27.72
ADAMTS-19	**ADAMTS19**	169	9.19
EV15L	**EVI5L**	168	37.83
TYRO10	**DDR2**	168	88.39
DR3 / TNFRSF25	**TNFRSF25**	168	1.74
MMP-24 / MT5-MMP	**MMP24**	167	24.27
APC	**APC**	167	12.02
NRG3	**NRG3**	166	48.64
AFP	**AFP**	166	5.30
Netrin G2	**NTNG2**	166	59.40

MMP-2	**MMP2**	165	39.14
NF1	**NF1**	165	14.14
MMP-11 /Stromelysin-3	**MMP11**	164	42.15
IL-17B R	**IL17RB**	163	34.09
LRG1	**LRG1**	163	13.79
Kremen-1	**KREMEN1**	163	41
CD97	**ADGRE5**	161	2.47
FAM3B	**FAM3B**	161	7.07
FGF-5	**FGF5**	159	15.14
Integrin alpha V	**ITGAV**	159	56.21
Endothelin Receptor A	**EDNRA**	159	36.06
IL-10	**IL10**	159	30.65
IGFBP-4	**IGFBP4**	158	13.73
Haptoglobin	**HP**	158	47.02
Bax	**BAX**	157	10.90
PTPRD	**PTPRD**	157	51.62
Artemin	**ARTN**	156	37.07
hCG alpha	**CGA**	156	38.89
Endostatin	**COL18A1**	155	41.18
GADD45A	**GADD45A**	155	25.81
CNDP1	**CNDP1**	154	9.55
Siglec-9	**SIGLEC9**	153	51.25
TSH	**TSHB**	153	71.06

ProSAAS	**PCSK1N**	153	55.15
FGF-20	**FGF20**	153	6.69
Caspase-8	**CASP8**	153	44.19
CD59	**CD59**	153	12.37
TRADD	**TRADD**	153	68.24
Hck	**HCK**	153	33.23
FOXN3	**FOXN3**	152	23.33
ROCK1	**ROCK1**	150	59.04

Supplemental Table 2. Complete list of proteins in ASC-EVs.

References

1. Cavallari C, Ranghino A, Tapparo M, Cedrino M, Figliolini F, Grange C, Giannachi V, Garneri P, Deregibus MC, Collino F, Rispoli P, Camussi G, Brizzi MF. Serum-derived extracellular vesicles (EVs) impact on vascular remodeling and prevent muscle damage in acute hind limb ischemia. *Sci Rep*. 2017. doi:10.1038/s41598-017-08250-0.
2. Ranghino A, Cantaluppi V, Grange C, Vitillo L, Fop F, Biancone L, Deregibus MC, Tetta C, Segoloni GP, Camussi G. Endothelial progenitor cell-derived microvesicles improve neovascularization in a murine model of hindlimb ischemia. *Int J Immunopathol Pharmacol*. 2012. doi:10.1177/039463201202500110.
3. Togliatto G, Trombetta A, Dentelli P, Cotogni P, Rosso A, Tschöp MH, Granata R, Ghigo E, Brizzi MF. Unacylated ghrelin promotes skeletal muscle regeneration following hindlimb ischemia via SOD-2-mediated miR-221/222 expression. *J Am Heart Assoc*. 2013. doi:10.1161/JAHA.113.000376.

4. Penna C, Tullio F, Femminò S, Rocca C, Angelone T, Cerra MC, Gallo MP, Gesmundo I, Fanciulli A, Brizzi MF, Pagliaro P, Alloatti G, Granata R. Obestatin regulates cardiovascular function and promotes cardioprotection through the nitric oxide pathway. *J Cell Mol Med*. 2017. doi:10.1111/jcmm.13277.

Major Resources Tables

Animals (in vivo studies)

Species	Vendor or Source	Background Strain	Sex
Mus musculus	Charles river laboratories	C57BL/6J	male

Animal breeding: Not available

Antibodies

Target antigen	Vendor or Source	Catalog #	Working concentration	Lot # (preferred but not required)
Neuregulin-1	Raybiotech	AA-BL-WB-NRG1	1μg/ml	*
CD31	Santa Cruz	SC-1506	1μg/ml	C0514
CD14	PharMingen	553738	1μg/ml	M074466
PCNA	Santa Cruz	SC-56	1μg/ml	G3115
CD63	Santa Cruz	SC-15363	1μg/ml	*
MyoD	Santa Cruz	SC-304	1μg/ml	B2410
Myogenin	Santa Cruz	SC-576	1μg/ml	B1510
CdK6	Santa Cruz	SC-7961	1μg/ml	*
pho-p38MAPK	Santa Cruz	SC-166182	1μg/ml	*
p38MAPK	Santa Cruz	SC-535	1μg/ml	*
Cyclin D1	Santa Cruz	SC-246	1μg/ml	A0814
p-BLC-2	Santa Cruz	SC-377576	1μg/ml	*
Bcl-XL	Santa Cruz	SC-8392	1μg/ml	*
β-Actin	Santa Cruz	SC-47778	1μg/ml	*
Vinculin	Santa Cruz	SC-7648	1μg/ml	C2913

* We used different lots of antibody

Cultured Cells

Name	Vendor or Source	Sex (F, M, or unknown)
ASC (human adipose-derived stem cells)	Lonza	M
C2C12 (mouse myoblast cell line)	ATCC	Unknown
HMEC-1 (human dermal microvascular endothelium)	ATCC	M
SC (mouse muscle satellite cells)	Gastrocnemius muscle (C57BL/6J mice)	M